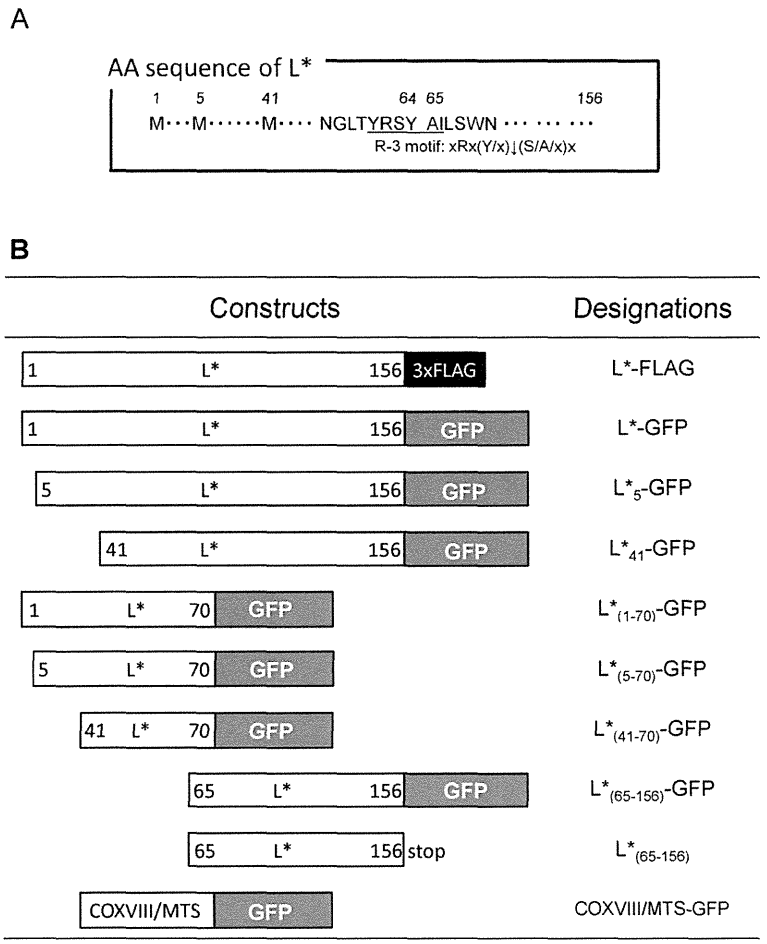

Fig. 1. Amino acid (AA) sequence of L* and diagrams of truncated L*–GFP fusion protein. (A) The positions of methionine (AA 1, 5, and 41) and R-3 motif (AA 61–66 [xRx(Y/x)(S/A/x)x (Schneider et al., 1998)]) on L*. (B) Diagram of FLAG- or GFP-fused L*. Full-length L* is fused with FLAG or GFP at the C-terminus. Truncated L*s are also fused with GFP at the C terminus. $L^*_{(65-156)}$ is co-expressed with $L^*_{(1-70)}$–GFP described in Section 2. A mitochondrial targeting signal of cytochrome *c* oxidase subunit VIII (COX VIII) is also fused with GFP at the C-terminus. Right column represents the designation of each construct.

expressing BHK-21 cells and tested the possibility that N-terminal sequence of L* may contain an MTS.

2. Materials and methods

2.1. Cell culture

BHK-21 cells, a baby hamster kidney-derived fibroblast cell line, were maintained in Eagle's minimum essential medium (MEM) (Nissui, Tokyo, Japan) supplemented with 5% newborn calf serum (CS) (Invitrogen, Carlsbad, CA) and 0.03% L-glutamine. Transfectants were maintained in MEM supplemented with 5% CS, 0.03% L-glutamine and 0.5 mg/ml of G418 (Nacalai tesque, Kyoto, Japan) (maintenance medium). Co-transfectant was maintained in the maintenance medium supplemented with 0.5 mg/ml of zeocin (Invitrogen, Carlsbad, CA).

2.2. Plasmid constructs

The full-length L* coding region of DA strain composing of 156 AA residues was amplified from a full-length cDNA of DA strain, pDAFL3 (Roos et al., 1989), by PCR. L* fragment was inserted into *Eco*RI and *Bam*HI sites of FLAG-tag mammalian expression vector, p3×FLAG-CMV-14 (Sigma–Aldrich Biotechnology, St. Louis, MO), designated L*–FLAG. Other constructs were expressed as green fluorescent protein (GFP) fusion protein using GFP fusion protein expression vector, pEGFP-N1 (Clontech, Mountain View, CA). Since pEGFP-N1 has a kozak sequence and a starting codon between multiple cloning site and GFP coding region, these sequences were deleted to avoid the independent expression of GFP (modified-pEGFP-N1). L* fragment was inserted into *Eco*RI and *Bam*HI sites of modified-pEGFP-N1, designated L*-GFP. The other truncated L* fragments were amplified from pDAFL3 by PCR and inserted into *Eco*RI and *Bam*HI sites of modified-pEGFP-N1. The detail of truncated L* fragments was as follows: constructs containing 5–156 and 41–156 AA residues of L* were designated L^*_5–GFP and L^*_{41}–GFP, respectively. Constructs containing N-terminal segments (1–70, 5–70 and 41–70 AA residues) of L* were designated $L^*_{(1-70)}$–GFP, $L^*_{(5-70)}$–GFP and $L^*_{(41-70)}$–GFP, respectively. C-terminal segment (65–156 AA residues) of L* was designated $L^*_{(65-156)}$–GFP.

An MTS of cytochrome *c* oxidase subunit VIII (COX VIII) was cloned by RT-PCR using RNA extracted from Jurkat cells according to the published data (Rizzuto et al., 1989, 1995). The products were inserted into *Eco*RI and *Bam*HI sites of modified-pEGFP-N1, designated COXVIII/MTS-GFP. C-terminal segment (65–156 AA residues) containing stop codon (TAG) was also amplified from pDAFL3 by PCR and inserted into *Hind*III and *Bam*HI sites of pcDNA4/TO vector (Invitrogen), designated $L^*_{(65-156)}$, for co-expression analysis.

2.3. Stable transfection

BHK-21 cells were transfected with each vector described above using Lipofectamine 2000 (Invitrogen) according to the manu-

facturer's instructions. After 24 h, 1.0 mg/ml of G418 was added to the medium (selective medium). Cells continued to cultivate in the selective medium for about 2 weeks. Surviving cells were cultured in maintenance medium. $L^*_{(1-70)}$–GFP-expressing BHK-21 cells were co-transfected with $L^*_{(65-156)}$ using Lipofectamine 2000. After 24 h, 0.5 mg/ml of zeocin was added to the maintenance medium. Co-transfected cells continued to cultivate in the selective medium containing G418 (0.5 mg/ml) and zeocin (0.5 mg/ml) for about 10 days. Surviving cells were cultured in the maintenance medium containing 0.5 mg/ml of zeocin.

2.4. Fluorescence microscopy

L^*–FLAG-expressing BHK-21 cells were seeded onto cover glasses coated by poly-L-lysine in 35 mm dish at a density of 50% confluency and cultured overnight. Cells were washed in phosphate buffered saline (PBS) and then stained by MitoTracker Red CMXRos (Invitrogen) according to the manufacturer's instructions. Briefly, cells were incubated in the maintenance medium containing 200 nM MitoTracker Red CMXRos for 30 min. Following two washes in PBS, cells were fixed in 10% formalin at 37 °C for 15 min. Then after two PBS washes, cells were permeabilized with 0.25% Triton X-100 for 10 min at room temperature and blocked with 5% bovine serum albumin in PBS for 1 h at room temperature. Cells were incubated with monoclonal anti-FLAG antibody (M2) (Sigma–Aldrich Biotechnology) at room temperature for 2 h. After three washes with PBS, cells were incubated with an FITC-conjugated anti-mouse IgG (Vector Laboratories, Inc., Burlingame, CA) for 1 h at room temperature. Stained cells were observed by a fluorescence microscope (Axiovision, Carl Zeiss).

GFP-fusion protein-expressing BHK-21 cells were seeded onto 35 mm glass bottom dish (Greiner bio-one, Frickenhausen, Germany) at a density of 50% confluency and cultured overnight. Cells were washed in PBS and then stained by MitoTracker Red CMXRos as described above. After two washes in PBS, cells were observed by a fluorescence microscope. Photomicrographs were obtained at room temperature with a microscope equipped with a digital camera (Axiovision, Carl Zeiss).

2.5. Immunoblotting

Mitochondrial and cytosolic proteins were extracted from L^*–FLAG-expressing BHK-21 cells, $L^*_{(65-156)}$–GFP-expressing BHK-21 cells and empty vector-transfected BHK-21 cells using ProteoExtract Cytosol/Mitochondria Fractionation Kit (Calbiochem, Darmstadt, Germany) according to the manufacturer's instructions. Briefly, 3×10^7 cells were homogenized in supplied cytosol extraction buffer mix. Homogenates were centrifuged at $700 \times g$ for 10 min at 4 °C. Supernatants were subsequently separated into cytosolic fraction and mitochondrial pellets by centrifugation at $10{,}000 \times g$ for 30 min at 4 °C. Mitochondrial pellets were lysed in supplied mitochondria extraction buffer mix (mitochondrial fraction). Mitochondrial and cytosolic extracts were separated by sodium dodecyl sulfate-15% polyacrylamide gel electrophoresis, and transferred onto a polyvinylidene difluoride membrane (Millipore, Billerica, MA). The membrane was blocked with 5% skim milk in PBS-T (PBS containing 0.05% Tween 20) for 60 min and incubated at 4 °C for overnight with rabbit anti-L^* antibody (Obuchi et al., 2001), rabbit anti-cytochrome *c* oxidase subunit IV (COX IV) antibody (Cell Signaling Technology, Beverly, MA), mouse anti-β-actin antibody (Sigma–Aldrich Biotechnology) or mouse anti-β-tubulin antibody (Sigma–Aldrich Biotechnology) followed by incubation with horseradish peroxidase (HRP)-conjugated anti-rabbit IgG (Bio-Rad Laboratories, Hercules, CA) or HRP-conjugated anti-mouse IgG (Bio-Rad Laboratories) for 1 h. Signals were detected using ECL plus Western blotting detection reagents (GE Healthcare, Little Chalfont, UK) according to the manufacturer's instructions.

Table 1
The summary of subcellular localizations of GFP fusion proteins. The diagram of each GFP fusion protein is presented in Fig. 1B.

GFP fusion protein	Localization
L^*–GFP	Mitochondria
L^*_5–GFP	Mitochondria
L^*_{41}–GFP	Mitochondria
$L^*_{(1-70)}$–GFP	Cytosol
$L^*_{(5-70)}$–GFP	Mitochondria
$L^*_{(41-70)}$–GFP	Mitochondria
$L^*_{(1-70)}$–GFP + $L^*_{(65-156)}$	Mitochondria
$L^*_{(65-156)}$–GFP	Cytosol

3. Results

3.1. Mitochondrial localization of L^* and truncated L^*

To clarify the association between L^* and mitochondria, we analyzed the subcellular localization of L^* by immunocytochemistry. BHK-21 cells were stably transfected with L^*–FLAG as described in Section 2. As shown in Fig. 2A, L^*–FLAG (green) was localized to mitochondria probed by MitoTracker Red CMXRos (red). Furthermore, L^*–FLAG (green) was observed as the ring-shaped around the mitochondrion (red) although the anti-FLAG antibodies are known to penetrate mitochondria in 0.25% TritonX-100 permeated cells (Fig. 2A, insets). To further confirm the mitochondrial localization of L^*, we performed Western blotting analysis using the mitochondrial protein extracts. L^*–FLAG was detected in mitochondrial fraction, though it was not detected in the cytosolic fraction (Fig. 2B, upper panel). COX IV, which is a mitochondrial protein, was also detected only in the mitochondrial fraction (Fig. 2B, second panel from the top). On the other hand, β-tubulin was detected in both mitochondrial and cytosolic fractions (Fig. 2B, the bottom panel), though β-actin was mainly detected in the cytosolic fraction (Fig. 2B, third panel from the top). These results demonstrated that L^* is localized to mitochondria (Table 1) and suggested that the association of L^* and tubulin may occur on mitochondria.

In addition, we analyzed the subcellular localization of truncated L^*, L^*_5 and L^*_{41} since AUG5 and AUG41 could be potential start codons (van Eyll and Michiels, 2002). We used the GFP fusion protein in this analysis, since GFP fusion protein is a good tool for visualizing subcellular localizations of protein of interest in living cells without any fixation (Rizzuto et al., 1995). Localization of L^*–GFP (Fig. 1B) was also analyzed as a control. As shown in Fig. 3, both of L^*_5–GFP and L^*_{41}–GFP (Fig. 1B) were localized to mitochondria as well as L^*–GFP, suggesting that all three L^*s have the ability of mitochondrial targeting (Table 1). Additionally, the data using L^*–GFP were similar to those using L^*–FLAG.

3.2. Analysis of mitochondrial targeting signal of L^*

A PSORTII analysis of the AA sequence of L^* predicted a cleavage site of MTS between residues 64 and 65 that matched R-3 motif which is endopeptidase cleavage motif in mitochondrial targeting peptides (Fig. 1A). Since N-terminus sequence of L^* may have some effect(s) on its activity as described in Section 1, we next tested the possibility that N-terminal sequence of L^* may contain an MTS using the GFP fusion protein (Fig. 1B). As a positive control of mitochondrial targeting, GFP fused with MTS of COX VIII was prepared according to the published data (Rizzuto et al., 1995) (COXVIII/MTS-GFP). COXVIII/MTS-GFP was localized to mitochondria as expected (Fig. 4, top panel). $L^*_{(5-70)}$–GFP was

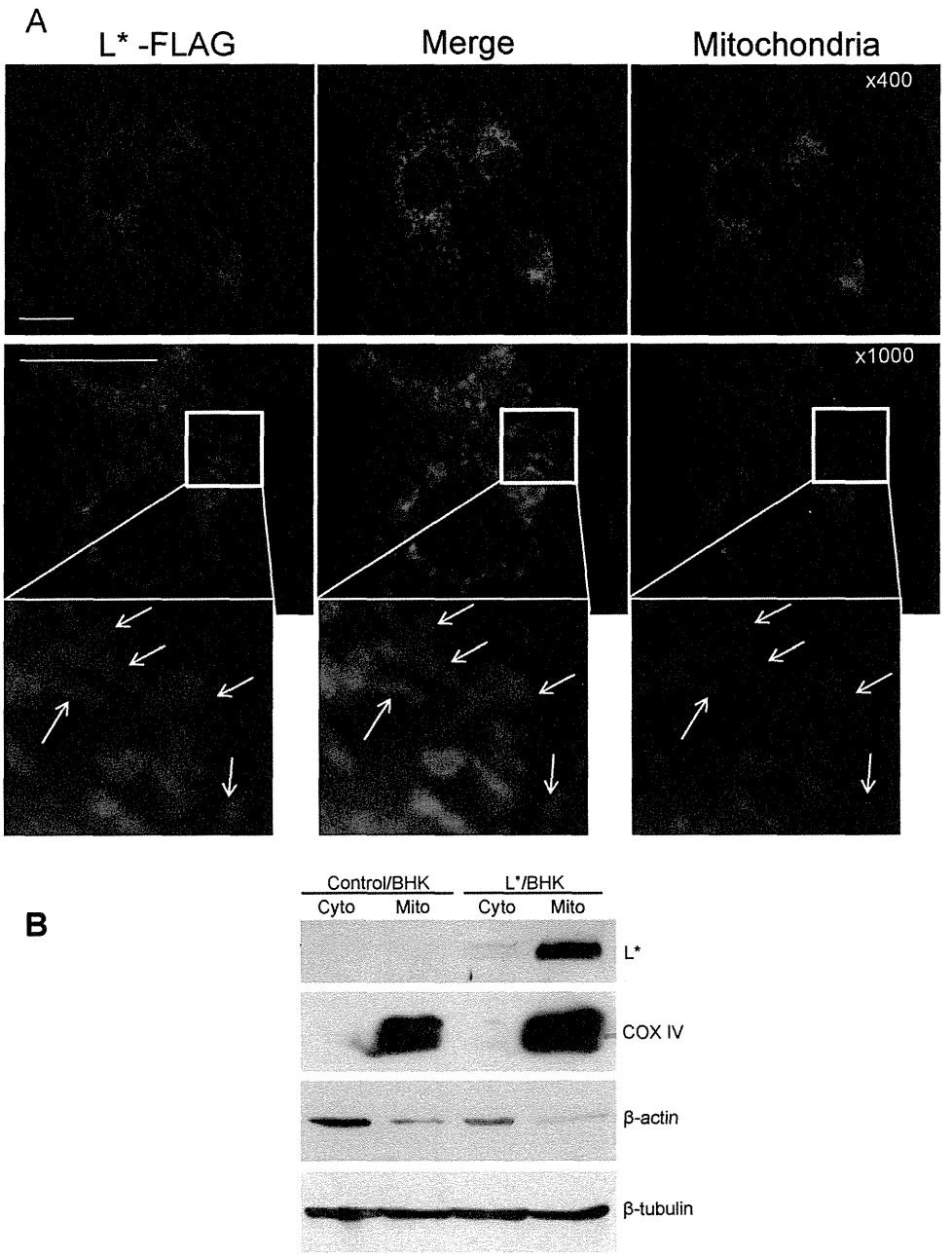

Fig. 2. Subcellular localization of L* in BHK-21 cells. (A) L* (green) was detected using anti-FLAG (M2) antibody and FITC-conjugated secondary antibody. Mitochondria (red) were stained with MitoTracker Red (Invitrogen). Merge represents merged images stained with anti-FLAG and MitoTracker Red. Lower panels show the insets. L* (green) was observed as the ring-shaped around the mitochondrion (red) (arrows). ×400 (Upper panels), ×1000 (middle panels). Bar = 20 μm. (B) Immunoblotting analysis of L*. Control/BHK and L*/BHK show empty vector-transfected BHK-21 cells and L*-FLAG expressing BHK-21 cells, respectively. Cyto and mito indicate cytosolic fraction and mitochondrial fraction, respectively. L* was detected in mitochondrial fraction with anti-L* antibody. β-Tubulin was detected in cytosolic and mitochondrial fractions. COX IV was detected as a control for mitochondrial fraction. β-Actin was detected as a control for cytosolic fraction. (For interpretation of the references to color in this figure legend, the reader is referred to the web version of the article.)

localized to mitochondria (Fig. 4, third panel from the top) as well as L^*_5–GFP. $L^*_{(41-70)}$–GFP was also localized to mitochondria (Fig. 4, lower panel) as well as L^*_{41}–GFP. Therefore, the sequence between AA positions 5 and 40 has little effects on the mitochondrial localization, suggesting that L* may have an MTS between AA positions 41 and 70. However, surprisingly, $L^*_{(1-70)}$–GFP was distributed in the cytosol contrary to the localization of L*–GFP (Fig. 4, second panel from the top). It is strongly suggested that $L^*_{(1-4)}$ may interfere the mitochondrial targeting of L*. The localization of each construct was summarized in Table 1.

3.3. Role of C-terminus of L* to mitochondrial targeting

If $L^*_{(1-4)}$ interferes in the mitochondrial targeting of L*, $L^*_{(65-156)}$ may reduce the interference in the mitochondrial targeting of L* by $L^*_{(1-4)}$ because L*–GFP was localized to mitochondria. To clarify the possibility that the intra- or inter-molecular interaction of L*, we next analyzed the effect of co-expression of $L^*_{(65-156)}$ on the distribution of $L^*_{(1-70)}$–GFP. As shown in Fig. 5A and Table 1, $L^*_{(1-70)}$–GFP was localized to mitochondria by co-expression with $L^*_{(65-156)}$. This result suggests that $L^*_{(65-156)}$ suppresses the interference in the mitochondrial targeting of L* by $L^*_{(1-4)}$. Therefore, it is suggested

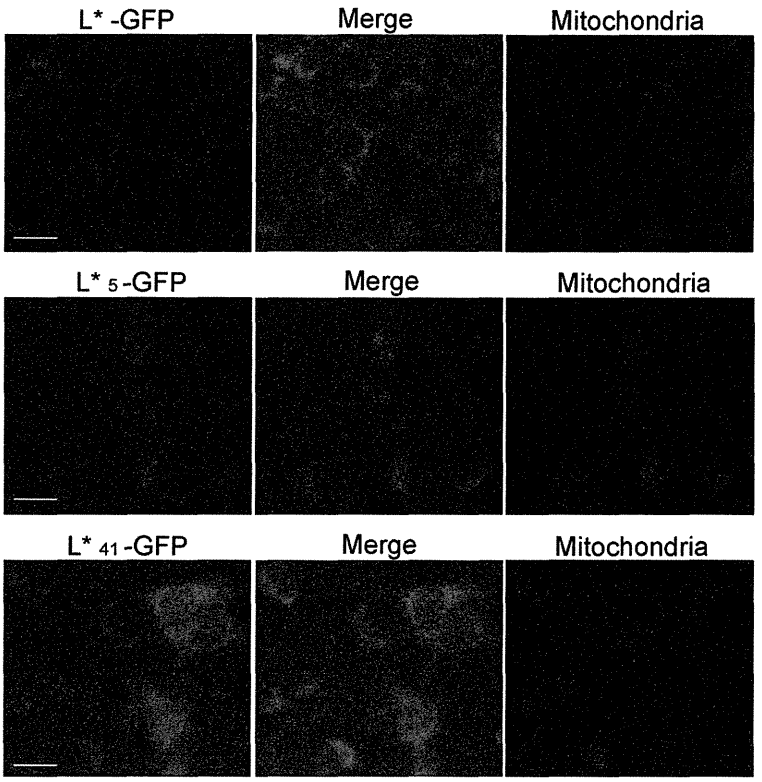

Fig. 3. Subcellular localization of truncated L* in BHK-21 cells. All of three sizes of L*s (GFP, green) were localized to mitochondria (MitoTracker Red, red), ×400. Bar = 20 μm. (For interpretation of the references to color in this figure legend, the reader is referred to the web version of the article.)

that the interaction between N- and C-terminal domains of L* may play an important role in the mitochondrial localization of L*.

Additionally, we analyzed the distribution of $L^*_{(65-156)}$–GFP in which the potential MTS is deleted (Fig. 5B and Table 1). Although the weak mitochondrial localization of $L^*_{(65-156)}$–GFP was observed in a part of cells (arrow head in Fig. 5B), it was mainly distributed in the cytosol. Western blotting, which was performed to confirm the localization, also demonstrated $L^*_{(65-156)}$–GFP was mainly detected in the cytosolic fraction although the faint signal was detected in the mitochondrial fraction (Fig. 5C). These results indicated that the MTS between AA positions 41 and 70 of L* is important for mitochondrial localization of L*.

4. Discussion

Apoptosis has been reported as a mechanism of cell death after infection with many viruses (Galluzzi et al., 2008; Roulston et al., 1999), such as human immunodeficiency virus, reovirus, hepatitis C virus, human papillomavirus and adenovirus. Apoptosis is the mechanism used by the host to limit viral infections. Viral infections affect the viability of the host cell through either inhibiting or promoting host cell apoptosis. Previous studies have shown that both GDVII and DA viruses of TMEV induce apoptosis *in vitro* and *in vivo* (Ghadge et al., 1998; Jelachich et al., 1999; Tsunoda et al., 1997). Therefore, apoptosis may play an important role in TMEV biological activities. Anti-apoptotic activity of L* was demonstrated by both 'loss of function' and 'gain of function' experiments (Ghadge et al., 1998; Himeda et al., 2005b). However, the precise mechanism(s) of inhibition of apoptosis by L* is unclear.

We previously reported that L* is co-localized with tubulin (Obuchi et al., 2001). Thereafter, it has been speculated that L* was associated with tubulin via the association with membrane or the formation of the complex, because L* has a strong hydrophobicity. In the present study, it was clearly demonstrated that L* and truncated L* are localized to mitochondria (Figs. 2 and 3, and Table 1). Furthermore, in the insets of Fig. 2A, L* (green) was observed around the mitochondrion (red), suggesting that L* is localized on the surfaces of mitochondria. On the other hand, the association of tubulin with mitochondria is well known (Heggeness et al., 1978; Hargreaves and Avila, 1985). In addition, it was reported that tubulin is an inherent component of mitochondrial membranes that interacts with the VDAC, the major channel of MOM (Carre et al., 2002; Rostovtseva et al., 2008). Therefore, the data of our previous study (Obuchi et al., 2001) may have shown the association of L* with tubulin on the surfaces of mitochondria. Recently, tubulin was reported to be a blocker of the mitochondrial VDAC, which is thought to be a key protein in mitochondria-mediated apoptosis (Rostovtseva et al., 2008). It was also reported that VDAC1 is involved in the release of not only cytochrome *c* but also Smac/Diablo and apoptosis inducing factor (AIF) (Shoshan-Barmatz et al., 2010). On the other hand, L protein of TMEV induces an intrinsic apoptosis in M1-D macrophage cells (Fan et al., 2009; Son et al., 2008, 2009). From these observations, it is suggested that L* may inhibit the intrinsic (mitochondria-mediated) apoptosis induced by TMEV infection through the regulation of VDAC activity by the association with tubulin on MOM.

In order to clarify the mechanism of mitochondrial targeting of L*, we next tested the possibility that N-terminal sequence of L* may have an MTS. Surprisingly, $L^*_{(1-70)}$–GFP was distributed in cytosol, although $L^*_{(5-70)}$–GFP and $L^*_{(41-70)}$–GFP were localized to mitochondria (Fig. 4 and Table 1). It is suggested that L* has an MTS between AA positions 41 and 70, and $L^*_{(1-4)}$ interferes in its mitochondrial targeting. More interestingly, co-expression of $L^*_{(65-156)}$ rescued the mitochondrial targeting of $L^*_{(1-70)}$–GFP (Fig. 5A and Table 1). This result indicated that $L^*_{(65-156)}$ suppressed the interference in the mitochondrial targeting of L* by $L^*_{(1-4)}$, because $L^*_{(65-156)}$–GFP, when solely expressed, was distributed in the cytosol (Fig. 5B and C and Table 1). $L^*_{(1-4)}$ may interfere in the

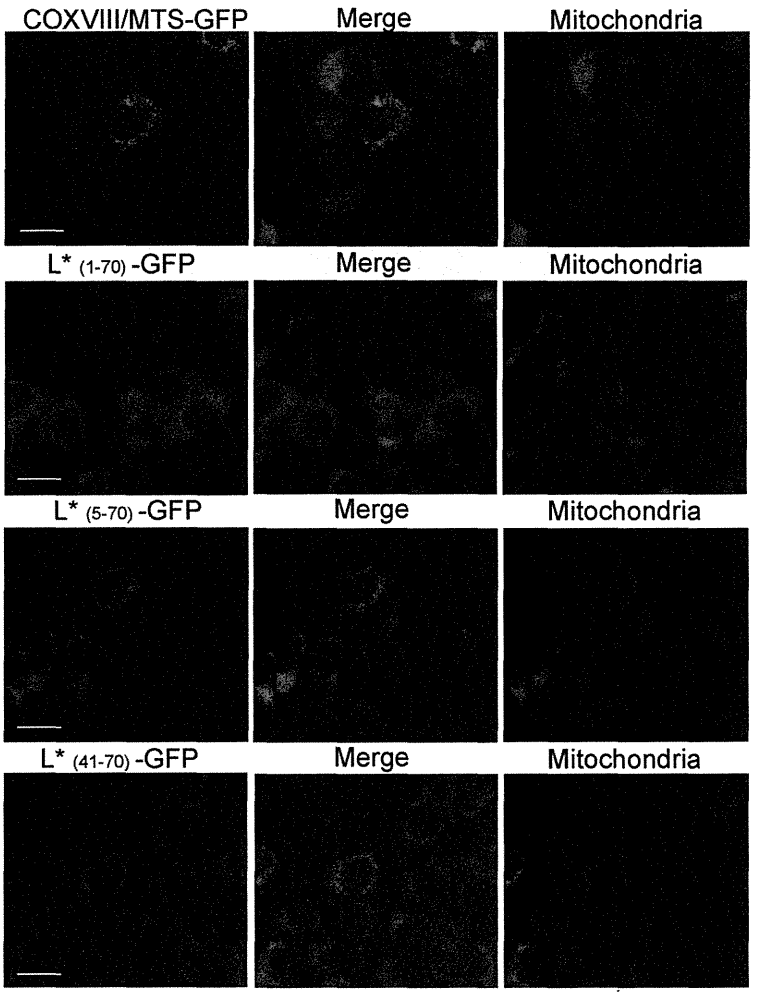

Fig. 4. Subcellular localization of L* –MTS fused-GFP in BHK-21 cells. $L^*_{(5-70)}$–GFP (green third panel from the top) and $L^*_{(41-70)}$–GFP (green, bottom panel) were localized to mitochondria (MitoTracker Red, red), although $L^*_{(1-70)}$–GFP (green, second panel from the top) was distributed in cytosol. COXVIII/MTS-GFP (green, top panel) was observed as a control for mitochondrial targeting, ×400. Bar = 20 μm. (For interpretation of the references to color in this figure legend, the reader is referred to the web version of the article.)

binding of cytosolic chaperones, mitochondrial import stimulation factor (MSF) or cytosolic heat-shock protein 70 (cHsp70), to L*–MTS due to the conformation change of $L^*_{(1-70)}$ induced by the absence of $L^*_{(65-156)}$. On the other hand, $L^*_{(65-156)}$ may suppress the interference by $L^*_{(1-4)}$ in the binding of L*–MTS with MSF or cHsp70. These results suggest that the intra- or inter-molecular interaction between N- and C-terminal domains of L* may play an important role in its mitochondrial localization as well as the intramolecular interaction of protein kinase C epsilon which is important for the regulation of its mitochondrial translocation (Budas et al., 2010; Schechtman et al., 2004).

L* is detected as a single band with the size of full length in DA-infected BHK cells (Ichinose-Asakura et al., 2010) although the R-3 motif is usually cleaved. It is, therefore, speculated that $L^*_{(41-70)}$ plays a role as an MTS without cleavage at the R-3 motif. It was also reported that the MTS sequences remain uncleaved in the cases of glutamine synthetase (Matthews et al., 2010) and others (Neupert, 1997). Since L* protein is not separated into the MTS and the mature protein, the generation of mutant L* which lacks the ability of localization to the mitochondria with keeping the anti-apoptotic activity is impossible. In order to further investigate whether L* localization to the mitochondria is imperative for inhibiting intrinsic apoptosis, the identification of residue(s) responsible for the MTS of L* are required. Stavrou et al. (2010) reported that L* AA 93 is important for TMEV persistence and demyelination *in vivo*. They further demonstrated that a change in L* AA 93 does not affect the anti-apoptotic activity of L*. Since L* AA 93 is not localized within the MTS in the present study, L* AA 93 is not an important residue for the mitochondrial translocation and anti-apoptotic activity of L*. The anti-apoptotic activity of L* may not be a sole factor, but one of factors determining TMEV persistence and demyelination. L* AA 93 could be one of the factors, but the issue remains to be clarified.

Recently, we reported that both L and L* of TMEV are required for virus growth in macrophage cells (Ichinose-Asakura et al., 2010). Furthermore, we found that L* inhibits L-induced apoptosis (Okuwa et al., 2010). Son et al. (2009) reported that activation of p53 was required for TMEV-induced apoptosis in M1-D macrophages. Interestingly, VDAC was identified as a putative partner of mitochondrial p53 in unstressed/proliferative cells (Ferecatu et al., 2009). From these observations, the following scenario is suggested: TMEV L induces the intrinsic apoptosis through the transcriptional activation of p53-dependent pro-apoptotic factors (Son et al., 2008, 2009). A part of p53 activated by TMEV L may be translocated to MOM and induce the release of apoptogenic factors into the cytosol by association with VDAC. On the other hand, L* may inhibit the release of apoptogenic factors from the mitochondria through blocking VDAC by association with tubulin on MOM. Therefore, further studies of the regulation system(s) of apoptotic cell death by L and L* are required to confirm the above-described hypothe-

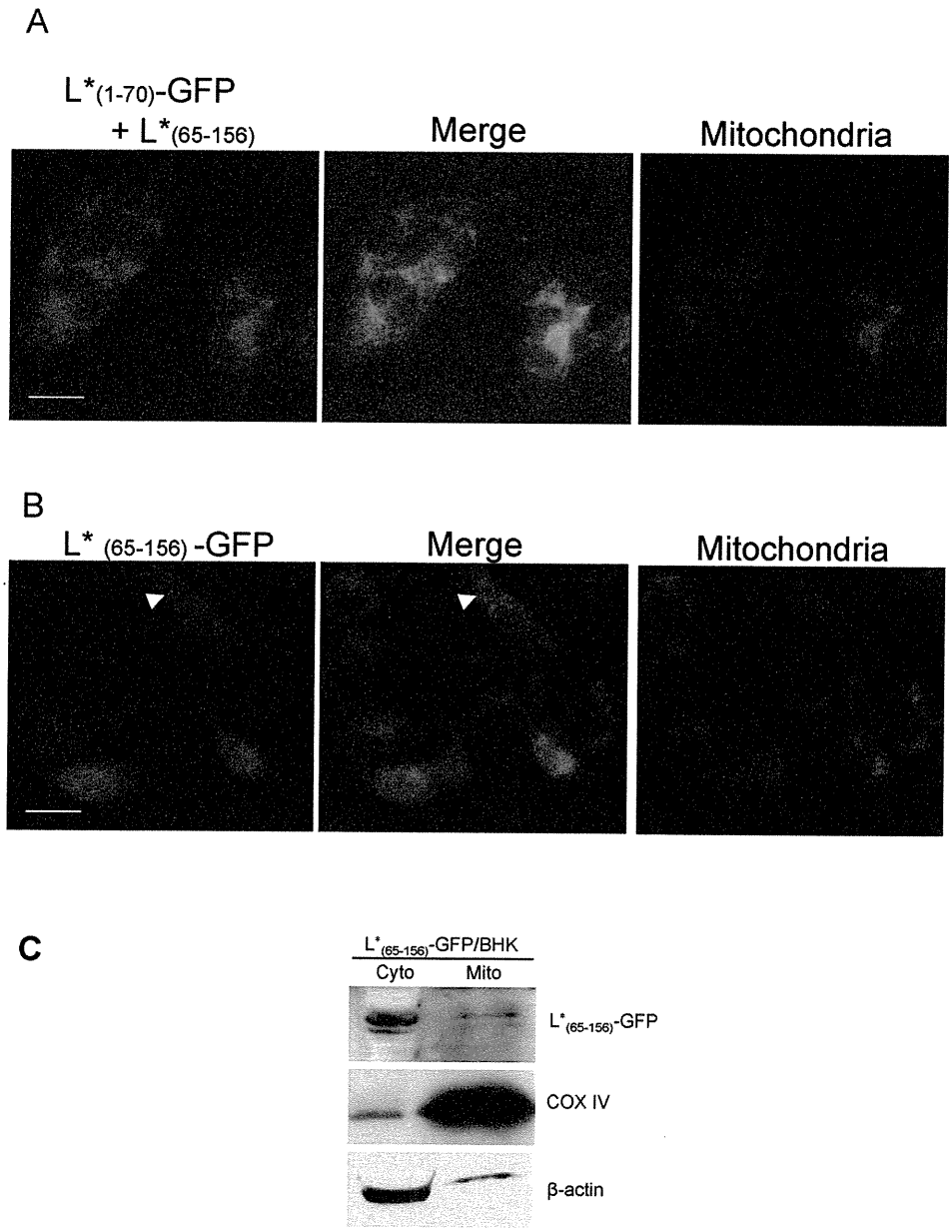

Fig. 5. (A) The change of subcellular localization of $L^*_{(1-70)}$–GFP by the co-expression with $L^*_{(65-156)}$. $L^*_{(1-70)}$–GFP was localized to the mitochondria by co-expression with $L^*_{(65-156)}$, ×400. Bar = 20 μm. (B) The subcellular localization of $L^*_{(65-156)}$–GFP. $L^*_{(65-156)}$–GFP, when solely expressed, was mainly distributed in the cytosol. However, the weak mitochondrial localization of $L^*_{(65-156)}$–GFP was observed in a part of cells (arrow head), ×400. Bar = 20 μm. (C) Immunoblotting with anti-L^* antibody. $L^*_{(65-156)}$–GFP was mainly detected in the cytosolic fraction. The faint signal of $L^*_{(65-156)}$–GFP was also detected in the mitochondrial fraction.

sis, leading to the elucidation of the pathomechanism(s) of TMEV persistence and TMEV-induced demyelination.

Acknowledgments

This work was supported in part by the Health and Labour Sciences Research Grant of Intractable Diseases (Neuroimmunological Diseases) from the Ministry of Health, Labour and Welfare of Japan, Grant-in-Aid for Scientific Research from the Ministry of Education, Culture, Sports, Science and Technology, Japan (22590421), and Grants of Promotion Research (S2009-4) and Assist KAKEN (K2010-16) from Kanazawa Medical University.

We thank Ms. Saito for her excellent technical assistance.

References

Budas, G.R., Churchill, E.N., Disatnik, M.-H., Sun, L., Mochly-Rosen, D., 2010. Mitochondrial import of PKCe is mediated by HSP90: a role in cardioprotection from ischemia and reperfusion injury. Cardiovasc. Res., doi:10.1093/cvr/cvq154.

Carre, M., Andre, N., Carles, G., Borghi, H., Brichese, L., Briand, C., Braguer, D., 2002. Tubulin is an inherent component of mitochondrial membranes that interacts with the voltage-dependent anion channel. J. Biol. Chem. 277, 33664–33669.

Drescher, K.M., Pease, L.R., Rodriguez, M., 1997. Antiviral immune responses modulate the nature of central nervous system (CNS) disease in a murine model of multiple sclerosis. Immunol. Rev. 159, 177–193.

Fan, J., Son, K., Arslan, S.Y., Liang, Z., Lipton, H.L., 2009. The Theiler's murine encephalomyelitis virus leader protein is the only nonstructural protein tested that induces apoptosis when transfected into mammalian cells. J. Virol. 83, 6546–6553.

Ferecatu, I., Bergeaud, M., Rodriguez-Enfedaque, A., Floch, N.L., Oliver, L., Rincheval, V., Renaud, F., Vallette, F.M., Mignotte, B., Vayssiere, J.-L., 2009. Mitochondrial localization of the low level p53 protein in proliferative cells. Biochem. Biophys. Res. Commun. 387, 772–777.

Galluzzi, L., Brenner, C., Morselli, E., Touat, Z., Kroemer, G., 2008. Viral control of mitochondrial apoptosis. PLoS Pathog. 4, e1000018.

Ghadge, G.D., Ma, L., Sato, S., Kim, J., Roos, R.P., 1998. A protein critical for a Theiler's virus-induced immune system-mediated demyelinating disease has a cell type-specific antiapoptotic effect and a key role in virus persistence. J. Virol. 72, 8605–8612.

Hargreaves, A.J., Avila, J., 1985. Localization and characterization of tubulin-like proteins associated with brain mitochondria: the presence of a membrane specific isoform. J. Neurochem. 45, 490–496.
Heggeness, M.H., Simon, M., Singer, S.J., 1978. Association of mitochondria with microtubules in cultured cells. Proc. Natl. Acad. Sci. U.S.A. 75, 3863–3866.
Himeda, T., Ohara, Y., Asakura, K., Kontani, Y., Murakami, M., Suzuki, H., Sawada, M., 2005a. A lentiviral expression system demonstrates that L* protein of Theiler's murine encephalomyelitis virus (TMEV) is essential for virus growth in a murine macrophage-like cell line. Virus Res. 108, 23–28.
Himeda, T., Ohara, Y., Asakura, K., Kontani, Y., Sawada, M., 2005b. A lentiviral expression system demonstrates that L* protein of Theiler's murine encephalomyelitis virus (TMEV) has an anti-apoptotic effect in a macrophage cell line. Microb. Pathog. 38, 201–207.
Ichinose-Asakura, K., Taniura, N., Himeda, T., Nojiri, M., Okuwa, T., Ohara, Y., 2010. Leader (L) of Theiler's murine encephalomyelitis virus (TMEV) is required for virus growth in a murine macrophage-like cell line. Virus Res. 147, 224–230.
Jelachich, M.L., Blamlage, C., Lipton, H.L., 1999. Differentiation of M1 myeloid precursor cells into macrophages results in binding and infection by Theiler's murine encephalomyelitis virus and apoptosis. J. Virol. 73, 3227–3235.
Kong, W.P., Roos, R.P., 1991. Alternative translation initiation site in the DA strain of Theiler's murine encephalomyelitis virus. J. Virol. 65, 3395–3399.
Lipton, H.L., Kumar, A.S.M., Trottier, M., 2005. Theiler's virus persistence in the central nervous system of mice is associated with continuous viral replication and a difference in outcome of infection of infiltrating macrophages versus oligodendrocytes. Virus Res. 111, 214–223.
Matthews, G.D., Gur, N., Koopman, W.J.H., Pines, O., Vardimon, L., 2010. Weak mitochondrial targeting sequence determines tissue-specific subcellular localization of glutamine synthetase in liver and brain cells. J. Cell Sci. 123, 351–359.
Michiels, T., Jarousse, N., Brahic, M., 1995. Analysis of the leader and capsid coding regions of persistent and neurovirulent strains of Theiler's virus. Virology 214, 550–558.
Monteyne, P., Bureau, J.-F., Brahic, M., 1997. The infection of mouse by Theiler's virus: from genetics to immunology. Immunol. Rev. 159, 163–176.
Neupert, W., 1997. Protein import into mitochondria. Annu. Rev. Biochem. 66, 863–917.
Obuchi, M., Odagiri, T., Asakura, K., Ohara, Y., 2001. Association of L* protein of Theiler's murine encephalomyelitis virus with microtubules in infected cells. Virology 289, 95–102.
Obuchi, M., Yamamoto, J., Uddin, N., Odagiri, T., Iizuka, H., Ohara, Y., 1999. Theiler's murine encephalomyelitis virus (TMEV) subgroup strain-specific infection in neural and non-neural cell lines. Microbiol. Immunol. 43, 885–892.
Okuwa, T., Taniura, N., Saito, M., Himeda, T., Ohara, Y., 2010. The opposite effects of two non-structural proteins of Theiler's murine encephalomyelitis virus (TMEV) regulates apoptotic cell death in BHK-21 cells. Microbiol. Immunol. 53, 639–643.
Oleszak, E.L., Chang, J.R., Friedman, H., Katsetos, C.D., Platsoucas, C.D., 2004. Theiler's virus infection: a model for multiple sclerosis. Clin. Microbiol. Rev. 17, 174–207.
Rizzuto, R., Nakase, H., Darras, B., Francke, U., Fabrizi, G.M., Mengel, T., Walsh, F., Kadenbach, B., DiMauro, S., Schon, E.A., 1989. A gene specifying subunit VIII of human cytochrome c oxidase is localized to chromosome 11 and is expressed in both muscle and non-muscle tissues. J. Biol. Chem. 264, 10595–10600.
Rizzuto, R., Brini, M., Pizzo, P., Murgia, M., Pozzan, T., 1995. Chimeric green fluorescent protein as a tool for visualizing subcellular organelles in living cells. Curr. Biol. 5, 635–642.
Roos, R.P., 2010. Pathogenesis of Theiler's murine encephalomyelitis virus-induces disease. Clin. Exp. Neuroimmunol. 1, 70–78.
Roos, R.P., Stain, S., Ohara, Y., Fu, J., Semler, B.L., 1989. Infectious cDNA clones of the DA strain of Theiler's murine encephalomyelitis virus. J. Virol. 63, 5492–5496.
Rostovtseva, T.K., Sheldon, K.L., Hassanzadeh, E., Monge, C., Saks, V., Bezrukov, S.M., Sackett, D.L., 2008. Tubulin binding blocks mitochondrial voltage-dependent anion channel and regulates respiration. Proc. Natl. Acad. Sci. U.S.A. 105, 18746–18751.
Roulston, A., Marcellus, R.C., Branton, P.E., 1999. Viruses and apoptosis. Annu. Rev. Microbiol. 53, 577–628.
Schechtman, D., Craske, M.L., Kheifets, V., Meyer, T., Schechtman, J., Mochly-Rosen, D., 2004. A critical intramolecular interaction for protein kinase Ce translocation. J. Biol. Chem. 279, 15831–15840.
Schneider, G., Sjöling, S., Wallin, E., Wrede, P., Glaser, E., von Heijne, G., 1998. Feature-extraction from endopeptidase cleavage sites in mitochondrial targeting peptides. Proteins 30, 49–60.
Shoshan-Barmatz, V., Keinan, N., Abu-Hamad, S., Tyomkin, D., Aram, L., 2010. Apoptosis is regulated by the VDAC1 N-terminal region and by VDAC oligomerization: release of cytochrome c, AIF and Smac/Diablo. Biochim. Biophys. Acta 1797, 1281–1291.
Son, K.-N., Becker, R.P., Kallio, P., Lipton, H.L., 2008. Theiler's virus-induced intrinsic apoptosis in M1-D macrophages is Bax mediated and restricts virus infectivity: a mechanism for persistence of a cytolytic virus. J. Virol. 82, 4502–4510.
Son, K.-N., Pugazhenthi, S., Lipton, H.L., 2009. Activation of tumor suppressor protein p53 is required for Theiler's murine encephalomyelitis virus-induced apoptosis in M1-D macrophages. J. Virol. 83, 10770–10777.
Stavrou, S., Baida, G., Viktorova, E., Ghadge, G., Agol, V.I., Roos, R.P., 2010. Theiler's murine encephalomyelitis virus L* amino acid position 93 is important for virus persistence and virus-induced demyelination. J. Virol. 84, 1348–1354.
Takano-Maruyama, M., Ohara, Y., Asakura, K., Okuwa, Y., 2006. Leader (L) and L* proteins of Theiler's murine encephalomyelitis virus (TMEV) and their regulation of the virus' biological activities. J. Neuroinflamm. 3, 19.
Takata, H., Obuchi, M., Yamamoto, J., Odagiri, T., Roos, R.P., Iizuka, H., Ohara, Y., 1998. L* protein of the DA strain of Theiler's murine encephalomyelitis virus is important for virus growth in a murine macrophage-like cell line. J. Virol. 72, 4950–4955.
Tsunoda, I., Kurtz, C.I.B., Fujinami, R.S., 1997. Apoptosis in acute and chronic central nervous system disease induced by Theiler's murine encephalomyelitis virus. Virology 228, 388–393.
van Eyll, O., Michiels, T., 2002. Non-AUG-initiated internal translation of the L* protein of Theiler's virus and importance of this protein for viral persistence. J. Virol. 76, 10665–10673.

Himeda et al. Virology Journal 2011, 8:110
http://www.virologyj.com/content/8/1/110

VIROLOGY JOURNAL

METHODOLOGY Open Access

The preparation of an infectious full-length cDNA clone of Saffold virus

Toshiki Himeda[1], Takushi Hosomi[2], Naeem Asif[3], Hiroyuki Shimizu[3], Takako Okuwa[1], Yasushi Muraki[1], Yoshiro Ohara[1*]

Abstract

The pathogenicity of Saffold virus (SAFV) among humans still remains unclear, although it was identified as a novel human cardiovirus in 2007. In order to encourage the molecular pathogenetic studies of SAFV, we generated an infectious cDNA clone of SAFV type 3 (SAFV-3). The present study demonstrated that the synthesis of the full-length infectious RNA by T7 RNA polymerase was terminated by a homologous sequence motif with the human preproparathyroid hormone (PTH) signal in the SAFV-3 genome. To obtain the infectious RNA using T7 promoter, a variant of T7 RNA polymerase, which fails to recognize the PTH signal, was useful. This study will provide a valuable technical insight into the reverse genetics of SAFV.

Background

The genus *Cardiovirus* belongs to the *Picornaviridae* family and is divided into two species: *Theilovirus* and *Encephalomyocarditis virus* (EMCV). *Cardiovirus* is thought to be associated with myocarditis, encephalitis and demyelinating disease in rodents [1,2]. EMCV is widely used as an experimental model for human diseases such as myocarditis, encephalitis and pancreatitis in rodents. TO subgroup strains of Theiler's murine encephalomyelitis virus (TMEV), a prototype of *Theilovirus*, serve as a mouse model for the human demyelinating disease, multiple sclerosis (MS) [3-5].

The existence of human cardiovirus has long been debated. In 2007, a novel cardiovirus, named Saffold virus (SAFV), was isolated as a human TMEV-like cardiovirus from an archived 1981 stool culture from an infant with a fever of unknown origin [6]. Subsequently, several groups identified Saffold-like cardioviruses, and eight genotypes of SAFV have been reported [6-10]. However, the pathogenicity of SAFV among humans remains unclear. In order to encourage the molecular pathogenetic studies of SAFV using a reverse genetics, the establishment of an infectious cDNA clone of SAFV is very important. In this study, we generated an infectious cDNA clone of SAFV-3 (the JPN08-404 strain), which is isolated from cerebrospinal fluid (CSF) of a patient with aseptic meningitis.

Results and discussion

The JPN08-404 strain was isolated in LLC-MK2 from the CSF of a patient with aseptic meningitis in 2008. Enterovirus and Parechovirus were negative by PCR analysis and neutralization test in this clinical sample (data not shown). The genomes of JPN08-404 (HQ902242) and SAFV-3 (FM240787) share 97% nucleotide and 99% amino acid identity. The homology clearly indicates that JPN08-404 belongs to genotype 3 of SAFV. In this study, we generated the full-length cDNA clone of JPN08-404 by using the specific primers carrying a T7 promoter as described in **Materials and methods**. This full-length cDNA clone was designated pSAF404 (Figure 1). The RNA synthesized from pSAF404 includes some additional sequences, which are GG residues at the 5' end and GCGGCC residues past the poly (A) tract at the 3' end. These extra nucleotides of pSAF404 at the 5' and 3' ends were similar to those of infectious cDNAs of poliovirus [11] and DA strain of TMEV [12].

HeLa cells were transfected with RNA, which is synthesized from pSAF404 (digested with *Not* I) by Thermo T7 RNA polymerase (TOYOBO), and the lysate of those HeLa cells was then inoculated on fresh HeLa cells. However, no cytopathic effect (CPE) was observed even after inoculating the cell lysate of these cells on

* Correspondence: ohara@kanazawa-med.ac.jp
[1]Department of Microbiology, Kanazawa Medical University School of Medicine, Ishikawa, Japan
Full list of author information is available at the end of the article

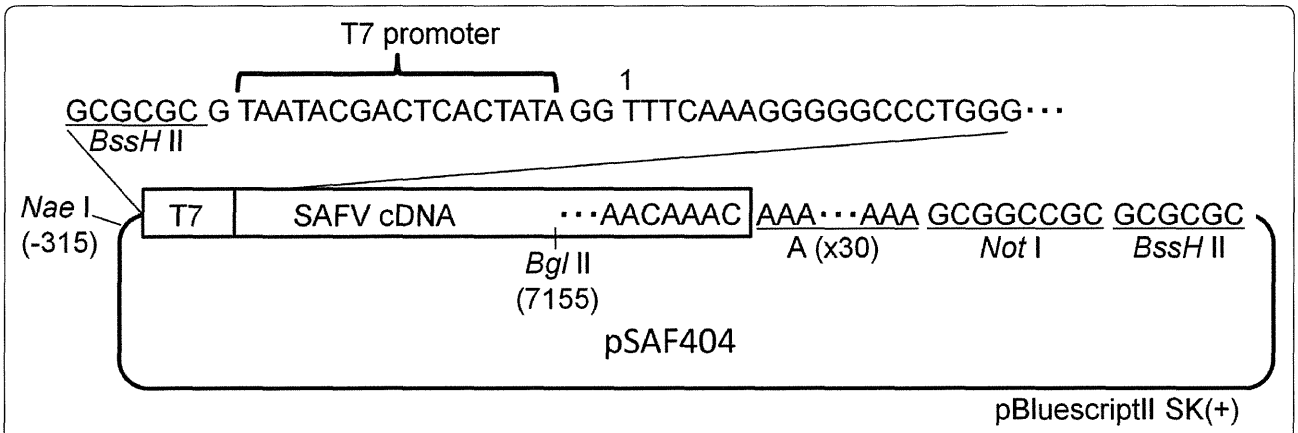

Figure 1 Diagram of pSAF404 containing a full-length JPN08-404 virus cDNA. A full-length cDNA of JPN08-404 virus (including 30 adenylate residues and *Not* I site at the 3' end) was inserted into pBluescriptII SK(+) at *Bss* HII site. The 5' end of JPN08-404 virus cDNA was placed two nucleotides downstream from the T7 promoter.

other fresh HeLa cells, suggesting that the infectious viral particles were not produced from HeLa cells transfected with RNA synthesized from pSAF404. To confirm the synthesis of a full-length RNA, electrophoresis was carried out using the transcripts from pSAF404 and pDAFL3, an infectious cDNA clone of DA strain of TMEV [12] as a control (Figure 2A). The transcripts from pSAF404 were apparently shorter than those from pDAFL3 (Figure 2A, lanes 1 and 5). Therefore, the failure in the production of the infectious viral particles

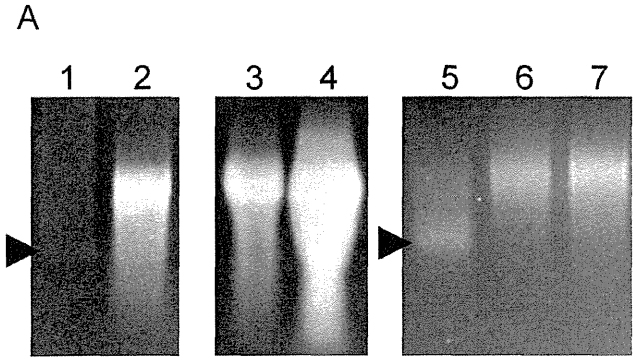

C

	PTH signal	
	conserved seq.	T-rich seq.
original seq	TATCTGTT	TGTTTTT
del PTH5	TACCTATT	CGTGTTC
del PTH2	TACCTATT	TGTTTTT

B

2601
AGGCTCTCTCAAT**TATCTGTT**TGTTTTTACTGGAAGCGCT

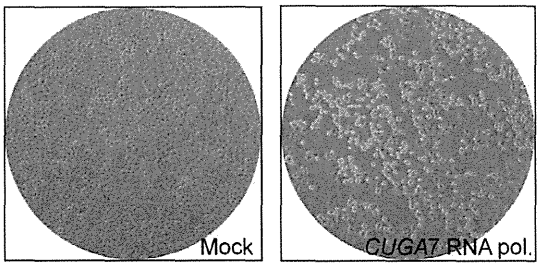

Figure 2 The termination of the transcription from pSAF404 caused by the PTH signal. A. RNAs synthesized from cDNA clones. Transcripts synthesized by Thermo T7 RNA polymerase from pSAF404 (lanes 1 and 5, arrow head) were shorter than the full-length RNA transcripts synthesized from pDAFL3, which is the infectious cDNA clone of DA strain of TMEV (lane 2). However, full-length RNAs were synthesized from pSAF404 (lane 3) and pDAFL3 (lane 4) by *CUGA* 7 RNA polymerase. Full-length RNAs were also synthesized by Thermo T7 RNA polymerase from the deletion mutants of the PTH signal; delPTH2 (lane 6) and delPTH5 (lane 7). B. PTH signal in the genome of JPN08-404. An underline indicates the conserved (bold) and T-rich sequences related to the PTH signal. 2601 is the number of nucleotides. C. The mutations to delete the PTH signal. Bold letters indicate mutations. These mutations do not change the amino acid sequences. D. Cytopathic effect induced by the infection of cDNA-derived virus. Right panel: cDNA-derived JPN08-404 virus infection; left panel: mock infection.

may be due to a premature termination during *in vitro* transcription. In order to further investigate the reason of transcriptional termination in pSAF404, the sequence of pSAF404 was compared in detail with that of pDAFL3. We identified a homologous sequence motif with the human preproparathyroid hormone (PTH) signal [13-15] within the sequence of pSAF404 (Figure 2B). The PTH signal, consisting of a conserved sequence (A/C/TATCTGTT) followed by a T rich sequence, is known as a class II site associated with the termination of transcription by bacteriophage T7 RNA polymerase [13-15]. Therefore, we next carried out the transcription from pSAF404 by using *CUGA* 7 RNA polymerase (NIPPON GENE), a variant of T7 RNA polymerase which fails to recognize the PTH signal (the manufacturer's instructions, personal communication). As a result, the synthesis of full-length RNA (⊠8 kb) from pSAF404 (Figure 2A, lane 3) was observed instead of the short-length RNA (Figure 2A, lane 1). However, the amount of the transcripts from pSAF404 was lower than that from pDAFL3 (Figure 2A, lanes 3 and 4). The T repeat of the 5' end of JPN08-404 may affect the transcriptional efficiency of bacteriophage RNA polymerase (the manufacturer's instructions). To further confirm whether the termination of transcription from pSAF404 is caused by the PTH signal, we generated the deletion mutants of PTH signal, delPTH2 and delPTH5 (Figure 2C). As expected, the synthesis of full-length RNAs from both delPTH2 and delPTH5 by Thermo T7 RNA polymerase were observed (Figure 2A, lanes 6 and 7). Therefore, it was demonstrated that the transcription from pSAF404 by T7 RNA polymerase was terminated by the PTH signal in the genome of JPN08-404. The amount of transcripts from delPTH5 was higher than that from delPTH2. The mutations of delPTH2 may be insufficient for the complete collapse of the PTH signal. Furthermore, the CPE was observed on HeLa cells transfected with RNA (10 μg) synthesized from pSAF404 by *CUGA* 7 RNA polymerase within 48 h. Since it was not clear whether it was caused by the infectious virus particles or by the transfected RNA, the freeze-thawing lysate of these cells was inoculated to another fresh HeLa cells. The CPE was then induced on those HeLa cells (Figure 2D), indicating that the infectious virus particles were present in the lysate. In addition, the direct sequencing of the recovered virus demonstrated that the sequence of VP1 coding region is identical to that of SAFV (JPN08-404). Therefore, evasion of the termination of RNA transcription at the PTH signal is essential for the synthesis of infectious JPN08-404 RNA by T7 RNA polymerase. Among the representative SAFV strains, SAFV-3 (FM240787, GU943514) and SAFV-6 (FJ463617) possess the complete PTH signal (conserved sequence and T rich sequence) at 2614 nt, at 2415 nt and at 6516 nt, respectively, although SAFV-1 (EF165067), SAFV-2 (FN999911, EU376394, EU681176, GU943518), SAFV-3 (EU681178, HM181997) and SAFV-5 (FJ463615) do not possess the complete PTH signal. Therefore, the termination of transcription by T7 RNA polymerase may be specifically observed in some SAFV-3 and SAFV-6 strains.

In the next step, growth kinetics of cDNA-derived JPN08-404 virus was analyzed by a standard plaque assay using HeLa cells. The titers of cell-free and cell-associated original JPN08-404 viruses reached a peak (1.7×10^7 and 4.8×10^6 PFU/ml, respectively) at 24 h after infection and gradually decreased thereafter (Figure 3A, left panel). The cDNA-derived JPN08-404 virus showed similar growth kinetics; reached a peak (cell-free: 1.2×10^7 PFU/ml, cell-associated: 5.0×10^6 PFU/ml) at 24 h after infection and gradually decreased thereafter (Figure 3A, right panel). The size of plaques of these viruses was almost similar (Figure 3B). These results suggested that the cDNA-derived virus has the biological activities similar to the original JPN08-404 virus.

Conclusions

In conclusion, the infectious cDNA clone of SAFV, e.g., pSAF404 generated in present study, is thought to be a powerful tool for the molecular pathogenetic studies of SAFV using a reverse genetics. However, to obtain the infectious RNA of some SAFV-3 strains using T7 promoter, T7 RNA polymerase ignoring the PTH signal (e.g. *CUGA* 7 RNA polymerase) or the deletion mutant of the PTH signal will be required. In order to generate the cDNA-derived SAFV without any artificial mutations, the combination of pSAF404 and T7 RNA polymerase, which fails to recognize the PTH signal, may be a useful tool. This study will provide a valuable technical insight into the reverse genetics of SAFV.

Materials and methods

Cells and viruses

HeLa cells, derived from human cervical carcinoma, were maintained in Dulbecco's modified Eagle's medium (DMEM, SIGMA) supplemented with 0.03% L-glutamine and 10% fetal bovine serum (FBS) containing 50 U/ml of penicillin and 50 μg/ml of streptomycin. LLC-MK2 cells, derived from rhesus monkey kidney epithelium, were maintained in Eagle's minimum essential medium (NISSUI) supplemented with 0.03% L-glutamine and 10% FBS containing 60 μg/ml of kanamycin. An SAFV strain, JPN08-404, was isolated in LLC-MK2 cells from the CSF (following removal of the cells by centrifugation) of a nine-year-old boy with aseptic meningitis in Kochi city, Japan, in 2008, and the isolate was identified as SAFV type 3 by sequence analysis of

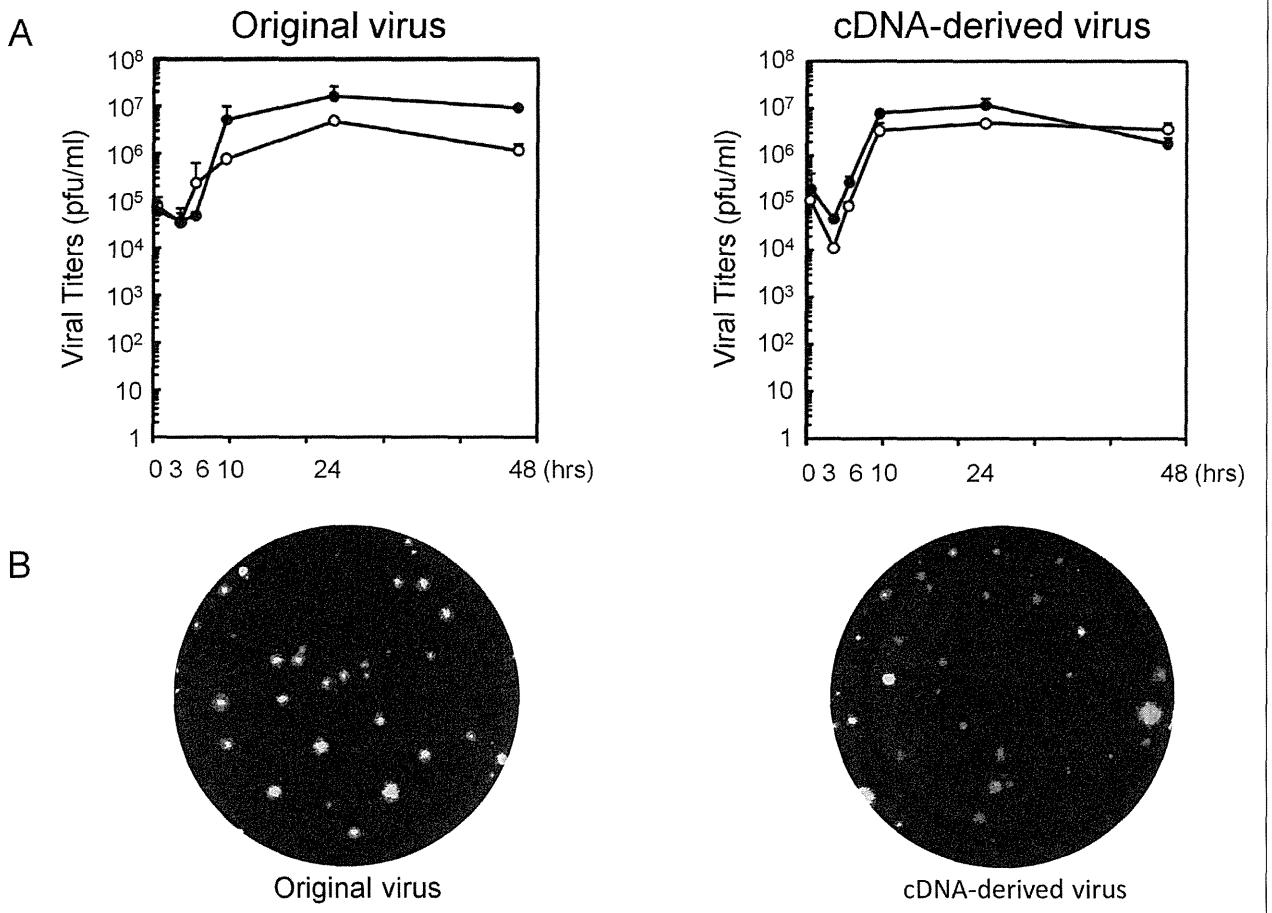

Figure 3 Characteristics of the cDNA-derived JPN08-404 virus. A: Growth kinetics of the original and cDNA-derived JPN08-404 viruses. Left panel: the original JPN08-404 virus. Right panel: the cDNA-derived JPN08-404 virus. The culture supernatants (closed circle) and the cells (open circle) were harvested at several time points indicated and assayed for titers by a standard plaque assay on HeLa cells. Titers shown are the means ± S.D. in three independent experiments. B: Plaque sizes of original and cDNA-derived JPN08-404 viruses. Left panel: the original JPN08-404 virus. Right panel: cDNA-derived JPN08-404 virus.

the VP1 region (data not shown). Thereafter, virus was propagated in HeLa cells, and the lysate was prepared by three freezing/thawing cycles to release virions. The titer of virus was determined by a standard plaque assay on HeLa cells.

Constructions of infectious cDNA clones

To obtain a full-length clone, viral RNA was extracted from JPN08-404 propagated in HeLa cells using RNeasy mini kit (QIAGEN) according to the manufacturer's instructions. Viral RNA was reverse-transcribed by ReverTra Ace (TOYOBO) with oligo dT(20) primer. The full-length clones were generated by PCR using KOD plus Neo (TOYOBO) with the following primer set; A forward primer, 5'-CATGCGCGCGTAATACGACTCACTATAGGTTTCAAAGGGGGCCCTGGG-3', A reverse primer, 5'-CATGCGCGCGCGGCCGCG TTCTCATTTC CAATTAAAAGC-3'. The forward primer contains the sequences of *Bss* HII site, T7 promoter, spacer (GG) and 5' end of SAFV-3 (FM207487), sequentially from 5' end. The reverse primer contains the sequences of 3' end of SAFV-3 (FM207487), *Not* I site and *Bss* HII site, sequentially from 3' end. PCR products were digested by *Bss* HII and then inserted into pBluescriptII SK(+) (STRATAGENE) digested by *Bss* HII. To remove the artificial mutations inserted during PCR reaction and cloning steps, the clone named pSAFL1 was reconstructed with other two clones according to the sequence of full-length viral genome of JPN08-404 (HQ902242) determined by direct sequencing and rapid amplification of cDNA ends (RACE). However, pSAFL1 did not contain the four nucleotides (5'-AAAC-3') located in 3'end of JPN08-404 and poly (A) sequences. Therefore, in order to obtain pSAF404, the clones including the fragment from *Bgl* II site (nt 7155) to poly (A) sequence with *Not* I site were generated by 3' RACE. *Bgl* II - *Not* I fragment of pSAFL1

was then replaced with the novel *Bgl* II - *Not* I fragment including the complete 3' end and 30 adenylate residues. The deletion mutants of PTH signal were generated by PCR using the specific primers including the mutations.

In vitro transcription and virus generation

pSAF404 and other plasmids (deletion mutants of the PTH signal) were linearized with *Not* I, and RNA transcripts were synthesized with Thermo T7 RNA polymerase (TOYOBO) or *CUGA* 7 RNA polymerase (NIPPON GENE). pDAFL3 [12] was linearized with *Xba* I, and RNA transcripts were synthesized with Thermo T7 RNA polymerase or *CUGA* 7 RNA polymerase. Then, HeLa cells were transfected with the transcripts derived from pSAF404 using Lipofectin (INVITROGEN) according to the manufacturer's instructions. The cultured cells and supernatants were collected after 48 hours, and viruses were prepared by three freezing/thawing cycles to release virions. The titers of viruses were determined by a standard plaque assay on HeLa cells.

Kinetics of virus growth in cells

The kinetics of virus growth of the original and the cDNA-derived viruses in HeLa cells was analyzed. The cells were seeded at a density of 5×10^5 cells in a 35-mm dish. After 24 h, the cells were infected with each virus at a multiplicity of infection of 5 PFU per cell. After virus adsorption at 37°C for 60 min, the cells were washed twice with Dulbecco's phosphate buffered saline, and incubated at 37°C in DMEM with 1% FBS. The cells and supernatants were collected at 0, 3, 6, 10, 24, and 48 h after infection and the cell-associated viruses were prepared by three freezing/thawing cycles from the cells. Cell-free and cell-associated viruses were titrated by a standard plaque assay on HeLa cells.

List of abbreviations used

CPE: cytopathic effect; CSF: cerebrospinal fluid; DMEM: Dulbecco's modified Eagle's medium; EMCV: Encephalomyocarditis virus; FBS: fetal bovine serum; PTH: preproparathyroid hormone; RACE: rapid amplification of cDNA ends; SAFV: Saffold virus; TMEV: Theiler's murine encephalomyelitis virus.

Acknowledgements

This work was supported in part by a Grant-in-Aid for Research on Emerging and Re-emerging Infectious Diseases and a Grant-in-Aid for the Promotion of Polio Eradication from the Ministry of Health, Labour and Welfare, Japan, the Health and Labour Sciences Research Grant of Intractable Diseases (Neuroimmunological Diseases) from the Ministry of Health, Labour and Welfare of Japan, Grant-in-Aid for Scientific Research from the Ministry of Education, Culture, Sports, Science and Technology, Japan (22590421), and Assist KAKEN (K2010-16) from Kanazawa Medical University.
We thank Ms. Saito for her excellent technical assistance.

Author details

[1]Department of Microbiology, Kanazawa Medical University School of Medicine, Ishikawa, Japan. [2]The Public Health Institute of Kochi Prefecture, Kochi, Japan. [3]Department of Virology II, National Institute of Infectious Diseases, Tokyo, Japan.

Authors' contributions

THi designed and performed the experiments and drafted the manuscript. THo performed the virus isolation. NA and HS determined the viral genome sequence. YM and TO supported the experiments of growth kinetics. All authors read and approved the final manuscript. YO supervised the work and edited the final version of this manuscript.

Competing interests

The authors declare that they have no competing interests.

Received: 28 January 2011 Accepted: 9 March 2011
Published: 9 March 2011

References

1. Brahic M, Bureau JF, Michiels T: **The genetics of the persistent infection and demyelinating disease caused by Theiler's virus.** *Annu Rev Microbiol* 2005, **59**:279-298.
2. Liang Z, Kumar ASM, Jones MS, Knowles NJ, Lipton HL: **Phylogenetic analysis of the species Theilovirus: Emerging murine and human pathogens.** *J Virol* 2008, **82**:11545-11554.
3. Oleszak EL, Chang JR, Friedman H, Katsetos CD, Platsoucas CD: **Theiler's virus infection: a model for multiple sclerosis.** *Clin Microbiol Rev* 2004, **17**:174-207.
4. Roos RP: **Pathogenesis of Theiler's murine encephalomyelitis virus-induces disease.** *Clin Exp Neuroimmunol* 2010, **1**:70-78.
5. Takano-Maruyama M, Ohara Y, Asakura K, Okuwa T: **Leader (L) and L* proteins of Theiler's murine encephalomyelitis virus (TMEV) and their regulation of the virus' biological activities.** *J Neuroinflammation* 2006, **3**:19.
6. Jones MS, Lukashov VV, Ganac RD, Schnurr DP: **Discovery of a novel human picornavirus in a stool sample from a pediatric patient presenting with fever of unknown origin.** *J Clin Microbiol* 2007, **45**:2144-2150.
7. Abed Y, Boivin G: **New Saffold cardioviruses in 3 children, Canada.** *Emerging Infectious Disease* 2008, **14**:834-836.
8. Blinkova O, Kappor A, Victoria J, Jones M, Wolfe N, Naeem A, Shaukat S, Sharif S, Alam MM, Angez M, Zaidi S, Delwart EL: **Cardioviruses are genetically diverse and cause common enteric infections in South Asian children.** *J Virol* 2009, **83**:4631-4641.
9. Blinkova O, Rosario K, Li L, Kappor A, Slikas B, Bernardin F, Breitbart M, Delwart E: **Frequent detection of highly diverse variants of cardiovirus, cosavirus, bocavirus, and circovirus in sewage samples collected in the United States.** *J Clin Microbiol* 2009, **47**:3507-3513.
10. Zoll J, Erkens Hulshof S, Lanke K, Verduyn Lunel F, Melchers WJ, Schoondermark-van de Ven E, Roivainen M, Galama JM, van Kuppeveld FJ: **Saffold virus, a human Theiler's-like cardiovirus, is ubiquitous and causes infection early in life.** *PLoS Pathog* 2009, **5**:e1000416.
11. van der Werf S, Bradley J, Wimmer E, Studier FW, Dunn JJ: **Synthesis of infectious poliovirus RNA by purified T7 RNA polymerase.** *Proc Natl Acad Sci USA* 1986, **83**:2330-2334.
12. Roos RP, Stein S, Ohara Y, Fu J, Semler BL: **Infectious cDNA clones of the DA strain of Theiler's murine encephalomyelitis virus.** *J Virol* 1989, **63**:5492-5496.
13. He B, Kukarin A, Temiakov D, Chin-Bow ST, Lyakhov DL, Rong M, Durbin RK, McAllister WT: **Characterization of an unusual, sequence-specific termination signal for T7 RNA polymerase.** *J Biol Chem* 1998, **273**:18802-18811.
14. Lyakhov DL, He B, Zhang X, Studier FW, Dunn JJ, McAllister WT: **Pausing and termination by bacteriophage T7 RNA polymerase.** *J Mol Biol* 1998, **280**:201-213.
15. Sohn Y, Kang C: **Sequential multiple functions of the conserved sequence in sequence-specific termination by T7 RNA polymerase.** *Proc Natl Acad Sci USA* 2005, **102**:75-80.

doi:10.1186/1743-422X-8-110
Cite this article as: Himeda *et al.*: **The preparation of an infectious full-length cDNA clone of Saffold virus.** *Virology Journal* 2011 **8**:110.

Plant Pathology & Microbiology

Ohara and Himeda, J Plant Pathol Microbiol 2011, 2:4
http://dx.doi.org/10.4172/2157-7471.1000e101

Editorial Open Access

A New Member of Cardiovirus: Unknown Pathogenicity to Humans

Yoshiro Ohara* and Toshiki Himeda

Department of Microbiology, Kanazawa Medical University School of Medicine Ishikawa, Japan

Members of the family *Picornaviridae* are nonenveloped viruses with a single-stranded RNA genome of positive polarity. 'Fields Virology' reads that the family contains many important human and animal pathogens and is composed of nine genera; aphthovirus, cardiovirus, enterovirus, erbovirus, hepatovirus, kobugvirus, parechovirus, rhinovirus, and teschovirus in the fifth edition [1]. The genus *Cardiovirus* contains Encephalomyocarditis virus (EMCV) and Theiler's murine encephalomyelitis virus (TMEV) and has long been believed to infect mainly rodents. However, in 2007, Saffold virus (SAFV) is identified from the stool sample with fever of unknown origin as a novel human cardiovirus [2]. Subsequently, SAFV was isolated from nasal and stool specimens from infants presenting with respiratory or gastrointestinal symptoms. In addition, the virus was isolated from the cerebrospinal fluid specimen of patient with aseptic meningitis. Since some seroepidemiological studies demonstrated that the seroprevalence to SAFV reaches > 90% in older than 24 months children and adults in several countries, SAFV is thought to be spread world-wide. Although several epidemiological studies have been reported up to now, they have failed to provide a clear answer of the relationship between SAFV and human diseases [3].

Animal experiments have been carried out in order to study the pathogenicity of SAFV, although SAFV does not infect rodents naturally. The experiments of different two groups suggest that SAFV is neurotropic in mice. Of special note is the presence of inflammation in the spinal cord white matter, because the closely related mouse cardiovirus, TMEV, causes a demyelinating central nervous system disease that resembles multiple sclerosis [3]. Therefore, the recombination between SAFV and TMEV, which could alter the host range, will be a serious problem to humans. However, Himeda et al. reported in the other issue of *J Plant Pathol Microbiol* that the recombination of capsid proteins between SAFV and TMEV did not occur [4]. Another important issue is that the major viral load following SAFV intraperitoneal inoculation is the pancreas. Several viruses in the family *Picornaviridae*, particularly Coxsackie B viruses have long been implicated in the etiology of type I diabetes. In addition, EMCV is known to induce pancreatitis and type I diabetes in rodents [3]. Recently, several European groups started the study to investigate the relationship between SAFV and type I diabetes. The answer to this issue awaits the data from them.

From these observations, the pathogenicity of SAFV still remains unclear, although the potential pathogenicity of SAFV to humans is thought to be varied (respiratory, gastrointestinal and neurological diseases and type I diabetes etc.). In order to clarify the pathogenicity of SAFV, the further epidemiological studies including the data of healthy persons as a control group is required. In addition, the researches of viral factors involved in the pathogenicity of SAFV using a reverse genetic technique [5] are needed. Furthermore, the identification of the receptor(s) for SAFV infection is also important in order to establish the transgenic mice as a novel animal model to study the pathogenicity of SAFV [3].

References

1. Vincent R. Racaniello VR (2007) Picornaviridae: the viruses and their replication, 795-838. *In* Knipe DM, Howley PM (ed.), *Fields Virology, 5th Ed.* Lippincott Williams & Wilkins, a Wolters Kluwer Business, Philadelphia.

2. Jones MS, Lukashov VV, Ganac RD, Schnurr DP (2007) Discovery of a novel human picornavirus in a stool sample from a pediatric patient presenting with fever of unknown origin. *J Clin Microbiol* 45: 2144-2150.

3. Himeda T, Ohara Y (2011) Saffold virus, a novel human cardiovirus with unknown pathogenicity. *J Virol* published online ahead of print on 23 Nov. 2011

4. Himeda T, Nojiri M, Okuwa T, Muraki Y, Ohara Y (2011) Reverse genetic analysis of the recombination in Theilovirus based on the infectious cDNA clones. *J Plant Pathol Microbiol* in press

5. Himeda T, Hosomi T, Asif N, Shimizu H, Okuwa T, et al. (2011) The preparation of an infectious full-length cDNA clone of Saffold virus. *Virol J* 8: 110.

***Corresponding author:** Yoshiro Ohara, M.D, Department of Microbiology, Kanazawa Medical University School of Medicine, 1-1 Uchinada, Ishikawa 920-0293, Japan, Tel: 81-76-286-221; Fax: 81-76-286-3961; E-mail: ohara@kanazawa-med.ac.jp

Received December 07, 2011; **Accepted** December 08, 2011; **Published** December 10, 2011

Citation: Ohara Y, Himeda T (2011) A New Member of Cardiovirus: Unknown Pathogenicity to Humans. J Plant Pathol Microbiol 2:e101. doi:10.4172/2157-7471.1000e101

Plant Pathology & Microbiology

Himeda et al. J Plant Pathol Microbiol 2011, 2:4
http://dx.doi.org/10.4172/2157-7471.1000112

Short Communication Open Access

Reverse Genetic Analysis of the Recombination in Theilovirus based on the Infectious cDNA Clones

Toshiki Himeda, Masafumi Nojiri, Takako Okuwa, Yasushi Muraki and Yoshiro Ohara*

Department of Microbiology, Kanazawa Medical University School of Medicine, Ishikawa, Japan

Abstract

Saffold virus (SAFV) which belongs to the species *Theilovirus* of the genus *Cardiovirus* of the family *Picornaviridae* is a novel human cardiovirus identified in 2007. However, the pathogenicity of SAFV to humans still remains unclear. Recent studies by the phylogenetic and recombination analyses of *Theilovirus* suggest that there are no recombination events between viruses of the different type (e.g. SAFV and Theiler's murine encephalomyelitis virus (TMEV)). Information on the recombination events of these viruses will be helpful to better understand the host specificity and pathogenicity of SAFV. In the present study, we performed the reverse genetic analysis to investigate the possibility of the recombination between SAFV and TMEV. The recombination of the capsid protein (VP1 and/or VP2) by reverse genetics between SAFV and TMEV did not happen, although the recombination of the non-capsid protein, L, occurred. These results strongly suggest that the shift of host range from rodents to humans or from humans to rodents by natural recombination of capsid protein(s) within Theiloviruses does not happen. The present results will provide the valuable information for the studies on the pathogenicity of SAFV.

Keywords: Theilovirus; TMEV; SAFV; Recombination

The genus *Cardiovirus* which belongs to the family *Picornaviridae* is divided into two species: *Theilovirus* and *Encephalomyocarditis virus* (EMCV). The natural hosts for Cardioviruses have been thought to be the rodents. However, in 2007, a human cardiovirus, designated Saffold virus (SAFV), was identified from an infant with a fever of unknown origin [1]. Its nucleotide sequences showed a strong similarity to Theiler-like rat virus (TRV), which was isolated from rats in Japan [2]. In the aid of phylogenetic analysis, SAFV was classified with TRV, Theiler's murine encephalomyelitis virus (TMEV) and Vilyuisk human encephalomyelitis virus (VHEV) into the species *Theilovirus* and eight genotypes of SAFV have been reported [1, 3-6].

The recombination is a common mechanism of evolution and antigenic variability for picornaviruses [7]. Recently, seven potential recombination events were reported by the phylogenetic and recombination analyses of *Theilovirus* species over the complete genomes [8]. According to this report, no recombination events were identified between viruses of the different type (e.g. SAFV and TMEV), although the potential recombination events were identified between the different SAFV strains. In addition, a previous study reported that there are apparently no recombination events between SAFV and TMEV [9]. To understand the host-specificity and pathogenicity of each virus, further information of the recombination within these viruses is valuable. Since previous studies [8,9] were only performed by using the computer software, in the present study, we performed the reverse genetic analysis by using the infectious cDNA clones to investigate whether the recombination between SAFV and TMEV potentially occurs or not.

The homology of capsid proteins (VP1, VP2, VP3 and VP4) between SAFV-3 (JPN08-404) and TMEV (DA and GDVII) was summarized in Table 1. The homology of amino acid sequence of VP1 is strikingly low between SAFV-3 and TMEV (56-57%). Furthermore, amino acid sequences of CD loop in VP1 and EF loop in VP2 of SAFV are markedly different from those of TMEV-DA (Figure 1). CD and EF loops have important roles to interact with the receptor of host cells [10]. If the recombination of these regions happened between SAFV and TMEV, the host range of this virus could be changed. Therefore, we generated the constructs for VP1 and/or VP2 recombinant viruses based on the infectious cDNA clone of SAFV-3, pSAF404 [11], the infectious cDNA clone of DA strain of TMEV (TMEV-DA), pDAFL3 [12], and the infectious cDNA clone of GDVII strain of TMEV (TMEV-GD), pGDVIIFL2 [13] to perform the reverse genetic analysis (Figure 2). pDAFL3 and pGDVIIFL2 were kindly provided from Dr. Raymond P. Roos (University of Chicago, IL). L protein (L) of TMEV is known to be important for cell-to-cell propagation [14], virus growth in macrophage cells and persistent infection [15]. However, it is not essential for virus production [14]. Therefore, the constructs for the L recombinant viruses were generated as a control for reverse genetics of recombinant viruses (Figure 2). Infectious RNAs transcribed from the constructs based on pSAF404 and the constructs based on pDAFL3 were transfected to HeLa and BHK-21 cells, respectively, as described previously [11]. On the cells transfected with synthesized RNA of SAFV-3, cytopathic effects (CPEs) were observed within 48 hours.

	homology (%)	
Capsid protein	vs TMEV-DA	vs TMEV-GDVII
VP4	68.1	68.1
VP2	70.1	68.6
VP3	79.3	81.0
VP1	56.7	56.0

This table shows the % of homologies of capsid proteins between SAFV-3 and TMEV (DA and GDVII). The homology of amino acid sequences was analyzed by genetyx ver. 10. Capsid proteins were arranged from the top according to the order from N-terminus of polyprotein

Table 1: The homologies of capsid proteins between SAFV-3 and TMEV (DA and GDVII).

***Corresponding author:** Yoshiro Ohara, M.D., Department of Microbiology, Kanazawa, Medical University School of Medicine, 1-1 Uchinada, Ishikawa 920-0293, Japan, Tel: 81-76-286-2211; Fax: 81-76-286-3961; E-mail: ohara@kanazawa-med.ac.jp

Received October 25, 2011; **Accepted** November 13, 2011; **Published** December 01, 2011

Citation: Himeda T, Nojiri M, Okuwa T, Muraki Y, Ohara Y (2011) Reverse Genetic Analysis of the Recombination in Theilovirus based on the Infectious cDNA Clones. J Plant Pathol Microbiol 2:112. doi:10.4172/2157-7471.1000112

```
CD loop (VP1)
 SAFV-3   LTPLPS---DIVNNSVLPEQE-RWISFASPTTQKPPYKTKQC
          ******   *     *       *    * *   *  ****
 TMEV-DA LTPLPSFCPDSTSGPVKTKAPVQWRWVRSGGTTNFPLMTKQC

EF loop (VP2)
 SAFV-3   PEFDTSNHSTEVEPRADTAFKVDANWQKHTQILTGHAYVNTTTKVNVPLALNHQNFW
          *** *                 *  *  *        **  *            * **** *
 TMEV-DA PEFYTGKGTKTGDMEPTDPFTMDTTWRAPQGAPTGYRY---DSRTGF-FAMNHQNQW
```

Figure 1: Amino acid similarity of CD and EF loops (the structures of the part of VP1 and VP2 proteins, respectively) between SAFV-3 (JPN08-404) and TMEV-DA. Asterisks indicate identical amino acid residue.

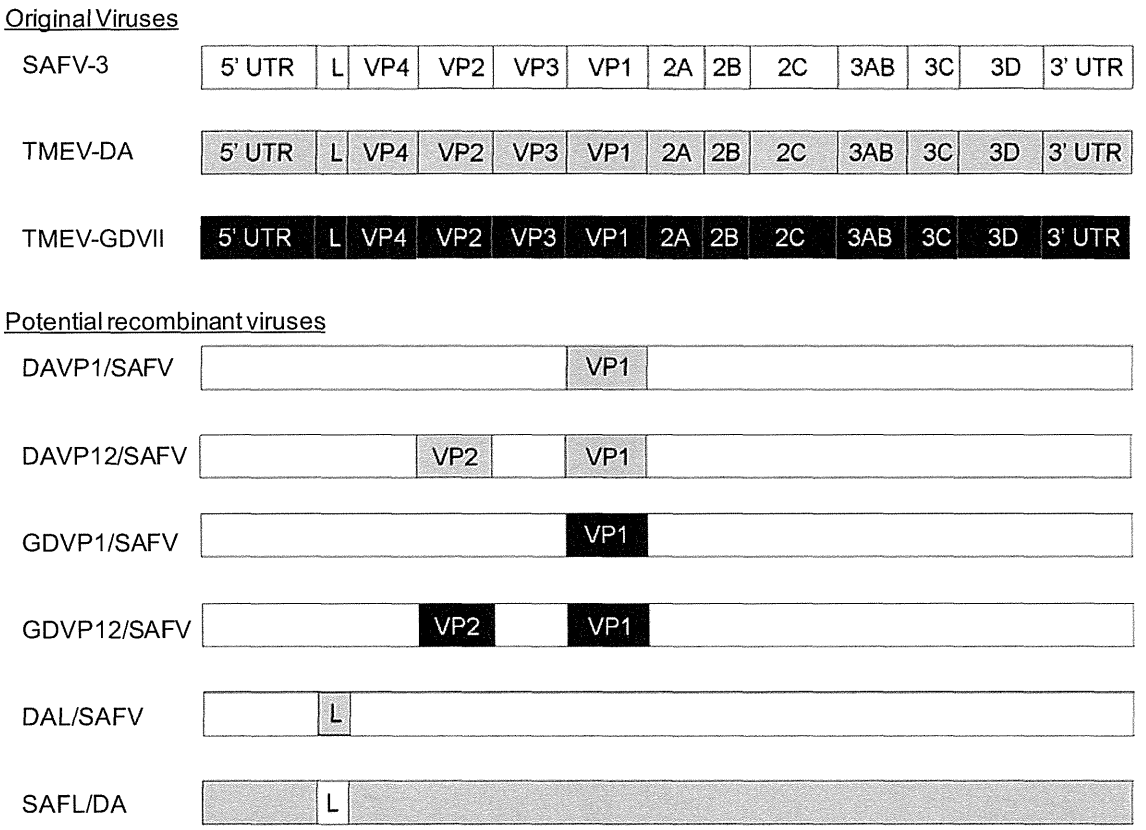

Figure 2: Diagrams of the constructs for recombinant viruses. The top three diagrams represent the genome structures of original viruses. White, gray and black boxes are SAFV-3, TMEV-DA and TMEV-GDVII, respectively. In DAVP1/SAFV, the VP1 coding region of SAFV-3 was replaced with that of TMEV-DA. In DAVP12/SAFV, the VP1 and VP2 coding regions of SAFV-3 were replaced with those of TMEV-DA. In GDVP1/SAFV and GDVP12/SAFV, the same recombination was designed. In DAL/SAFV, the L coding region from SAFV-3 was replaced with that of TMEV-DA. Vice versa recombination was designed in SAFL/DA. DAL/SAFV and SAFL/DA were generated as a control for reverse genetics of recombinant viruses.

The CPEs were also observed on the cells transfected with synthesized RNAs of DAL/SAFV, which is SAFV containing L of TMEV-DA. In the case of SAFL/DA, which is TMEV-DA containing L of SAFV, CPEs were also observed within 48 hours. These viruses were prepared by three freezing/thawing cycles, and then the plaques were isolated. The isolated viruses were propagated by several passages and the titers of recombinant viruses based on SAFV and TMEV-DA were determined by a standard plaque assay on HeLa and BHK-21 cells, respectively. The titers of SAFV-3 and SAFL/DA reached to 7.3×10^7 pfu/ml and 2.6×10^8 pfu/ml, respectively, after three passages. The titer of DAL/SAFV reached to 1.9×10^8 pfu/ml after six passages. This information suggests that the recombination of L between SAFV and TMEV could occur, although the propagation periods were not similar. The CPEs were not observed on the cells transfected with RNAs of SAFV which is recombined with VP1 and/or VP2 of TMEV (DAVP1/SAFV, DAVP12/SAFV, GDVP1/SAFV and GDVP12/SAFV) within 72 hours. Infectious viral particles of these recombinant viruses were not obtained even after three blind passages on HeLa and BHK-21 cells. Additionally, we analyzed the viral protein synthesis after transfection by Western blotting with mouse anti-VP1 antibody (DAmAb2) specifically reacted

to VP1 protein of TMEV-DA [16]. VP1 of TMEV-DA was detected in the lysate of the cells transfected with RNA of DAVP12/SAFV (data not shown). The result suggests that the translation from the transfected RNA and the maturation of VP1 by viral protease occurred. The reason for the lack of recombination could be 1) viral particles were not produced because of the failure of assembly by the changes of VP1 and/or VP2, 2) the recombinant viruses could not be attached to the receptor on HeLa and BHK-21 cells because of the collapse of the higher order structure of receptor binding regions by the changes of VP1 and/or VP2. Although further studies are required to confirm these propositions, it is strongly suggested that the recombination of VP1 and/or VP2 between SAFV and TMEV does not naturally occur.

In conclusion, the recombination of the capsid protein (VP1 and/or VP2) between viruses of the different type within *Theilovirus* species did not happen although the recombination of the non-capsid protein, L, occurred. These results agree with the previous reports by the phylogenetic and recombination analyses [8, 9]. From these observations, it is suggested that the changes of host range by natural recombination of capsid protein(s) between SAFV and TMEV do not occur. The present study will provide the valuable information for further research of the recombination among the species *Theilovirus*.

Acknowledgement

This work was supported by a Grant-in-Aid for Scientific Research from the Ministry of Education, Science, Sports and Culture (22590421), a Grant from the Neuroimmunological Research Committee of the Ministry of Health, Labor and Welfare, a Grant-in-Aid for Research on Emerging and Re-emerging Infectious Diseases and a Grant-in-Aid for the Promotion of Polio Eradication from the Ministry of Health, Labour and Welfare, Japan.

We thank Ms. Saito for her excellent technical assistance.

References

1. Jones MS, Lukashov VV, Ganac RD, Schnurr DP (2007) Discovery of a novel human picornavirus in a stool sample from a pediatric patient presenting with fever of unknown origin. J Clin Microbiol 45: 2144-2150.
2. Ohsawa K, Watanabe Y, Miyata H, Sato H (2003) Genetic analysis of a Theiler-like virus isolated from rats. Comp Med 53: 191-196.
3. Abed Y, Boivin G (2008) New Saffold cardioviruses in 3 children, Canada. Emerging Infectious Disease 14: 834-836.
4. Blinkova O, Kappor A, Victoria J, Jones M, Wolfe N, et al. (2009) Cardioviruses are genetically diverse and cause common enteric infections in South Asian children. J Virol 83: 4631-4641.
5. Blinkova O, Rosario K, Li L, Kappor A, Slikas B, et al. (2009) Frequent detection of highly diverse variants of cardiovirus, cosavirus, bocavirus, and circovirus in sewage samples collected in the United States. J Clin Microbiol 47: 3507-3513.
6. Zoll J, Erkens Hulshof S, Lanke K, Verduyn Lunel F, Melchers WJ, et al. (2009) Saffold virus, a human Theiler's-like cardiovirus, is ubiquitous and causes infection early in life. PLoS Pathog 5: e1000416.
7. Simmonds P (2010) Recombination in the evolution of Picornaviruses. Ehrenfeld E, Domingo E, Roos RP (ed.), The Picornaviruses. ASM Press, Washington, DC, 229-237.
8. Sun G, Zhang X, Yi M, Shao S, Zhang W (2011) Analysis of the genomic homologous recombination in Theilovirus based on complete genomes. Virol J 8: 439.
9. Drexler JF, Baumgart S, Luna LK, Stöcker A, Almeida PS, et al. (2010) Genomic features and evolutionary constraints in Saffold-like cardioviruses. J Gen Virol 91: 1418-1427.
10. Michiels T, Roos RP (2010) Theiler's Virus Central Nervous System Infection, In Ehrenfeld E, Domingo E, Roos RP (ed.), The Picornaviruses. ASM Press, Washington DC. 411-428.
11. Himeda T, Hosomi T, Asif N, Shimizu H, Okuwa T, et al. (2011) The preparation of an infectious full-length cDNA clone of Saffold virus. Virol J 8: 110.
12. Fu JL, Stein S, Rosenstein L, Bodwell T, Routbort M, et al. (1990) Neurovirulence determinants of genetically engineered Theiler viruses. Proc Natl Acad Sci USA 87: 4125-4129.
13. Roos RP, Stein S, Ohara Y, Fu JL, Semler BL (1989) Infectious cDNA clones of the DA strain of Theiler's murine encephalomyelitis virus. J Virol 63: 5492-5496.
14. Michiels T, Dejong V, Rodrigus R, Shaw-Jackson C (1997) Protein 2A is not required for Theiler's virus replication. J Virol 71: 9549-9556.
15. Himeda T, Ohara Y (2011) Roles of two non-structural viral proteins in virus-induced demyelination. Clin Exp Neuroimmunol 2: 49-58.
16. Nitayaphan S, Toth MM, Roos RP (1985) Localization of a neutralization site of Theiler's murine encephalomyelitis viruses. J Virol 56: 887-985.

Tyrosine Sulfation of the Amino Terminus of PSGL-1 Is Critical for Enterovirus 71 Infection

Yorihiro Nishimura, Takaji Wakita, Hiroyuki Shimizu*

Department of Virology II, National Institute of Infectious Diseases, Musashimurayama-shi, Tokyo, Japan

Abstract

Enterovirus 71 (EV71) is one of the major causative agents of hand, foot, and mouth disease, a common febrile disease in children; however, EV71 has been also associated with various neurological diseases including fatal cases in large EV71 outbreaks particularly in the Asia Pacific region. Recently we identified human P-selectin glycoprotein ligand-1 (PSGL-1) as a cellular receptor for entry and replication of EV71 in leukocytes. PSGL-1 is a sialomucin expressed on the surface of leukocytes, serves as a high affinity counterreceptor for selectins, and mediates leukocyte rolling on the endothelium. The PSGL-1–P-selectin interaction requires sulfation of at least one of three clustered tyrosines and an adjacent *O*-glycan expressing sialyl Lewis x in an N-terminal region of PSGL-1. To elucidate the molecular basis of the PSGL-1–EV71 interaction, we generated a series of PSGL-1 mutants and identified the post-translational modifications that are critical for binding of PSGL-1 to EV71. We expressed the PSGL-1 mutants in 293T cells and the transfected cells were assayed for their abilities to bind to EV71 by flow cytometry. We found that *O*-glycosylation on T57, which is critical for PSGL-1–selectin interaction, is not necessary for PSGL-1 binding to EV71. On the other hand, site-directed mutagenesis at one or more potential tyrosine sulfation sites in the N-terminal region of PSGL-1 significantly impaired PSGL-1 binding to EV71. Furthermore, an inhibitor of sulfation, sodium chlorate, blocked the PSGL-1–EV71 interaction and inhibited PSGL-1-mediated viral replication of EV71 in Jurkat T cells in a dose-dependent manner. Thus, the results presented in this study reveal that tyrosine sulfation, but not *O*-glycosylation, in the N-terminal region of PSGL-1 may facilitate virus entry and replication of EV71 in leukocytes.

Citation: Nishimura Y, Wakita T, Shimizu H (2010) Tyrosine Sulfation of the Amino Terminus of PSGL-1 Is Critical for Enterovirus 71 Infection. PLoS Pathog 6(11): e1001174. doi:10.1371/journal.ppat.1001174

Editor: Michael Farzan, Harvard Medical School, United States of America

Received April 1, 2010; **Accepted** September 30, 2010; **Published** November 4, 2010

Funding: *This work was supported by KAKENHI (Grant-in-Aid for Young Scientists (B), 21790452) from the Ministry of Education, Culture, Sports, Science and Technology, Japan (http://www.mext.go.jp/english/). Y.N. and H.S. were supported in part by a Grant-in-Aid for Research on Emerging and Re-emerging Infectious Diseases and a Grant-in-Aid for the Promotion of Polio Eradication, from the Ministry of Health, Labour and Welfare, Japan (http://www.mhlw.go.jp/english/index.html). The funders had no role in study design, data collection and analysis, decision to publish, or preparation of the manuscript.*

Competing Interests: The authors have declared that no competing interests exist.

* E-mail: hshimizu@nih.go.jp

Introduction

Enterovirus 71 (EV71) is a small, nonenveloped, positive-stranded RNA virus that belongs to human enterovirus species A of the genus *Enterovirus* in the family *Picornaviridae*. EV71 is a major causative agent of hand, foot, and mouth disease (HFMD), a common febrile disease affecting mainly young children. HFMD is characterized by a skin rash on the palms and soles, and ulcers on the oral mucosa. HFMD due to EV71 and other enteroviruses is usually mild and self-limited; however, EV71 infection may also cause severe neurological diseases including polio-like paralysis and fatal brainstem encephalitis in young children and infants (reviewed in [1,2]). Over the last decade, many EV71 outbreaks involving a number of fatal encephalitis cases have been reported throughout the world, especially in the Asia-Pacific region, including in Malaysia, Taiwan, Vietnam, and mainland China [2,3,4].

Using an expression cloning method by panning with a cDNA library from human Jurkat T cells, we recently identified human P-selectin glycoprotein ligand-1 (PSGL-1) as a functional cellular receptor for EV71 [5]. In addition, Yamayoshi et al. [6] identified scavenger receptor class B, member 2 (SCARB2) as another cellular receptor for EV71 by screening EV71-susceptible transformants after transfecting mouse L929 cells with genomic DNA from human RD rhabdomyosarcoma cells. SCARB2 is ubiquitously expressed on a variety of tissues and cells [7], whereas the tissue distribution of PSGL-1 is mainly limited to immune cells such as leukocytes and dendritic cells [8]. We have also demonstrated that some EV71 strains (PSGL-1–binding strain; EV71-PB) use PSGL-1 as the primary and functional receptor for infection of Jurkat T cells, but other EV71 strains (PSGL-1–non-binding strain; EV71-non-PB) do not, suggesting phenotypic differences in PSGL-1 usage among EV71 strains. Thus, the identification of two distinct cellular receptors for EV71, PSGL-1 and SCARB2, has provided important clues in the elucidation of the molecular basis of early virus-host interactions and pathogenesis of EV71. However, little is known about the biological significance of the two EV71 receptors.

PSGL-1 is a sialomucin membrane protein that is expressed as a homodimer comprised of two disulfide-linked subunits. Interaction of PSGL-1 with selectins and chemokines is a key event during early inflammation of immune cells [8,9,10,11]. The N-terminal region of PSGL-1 is critical for PSGL-1 binding to P-, E- and L-selectins, and post-translational modifications such as *O*-glycosylation and tyrosine sulfation in the N-terminal region of PSGL-1 contribute the efficient binding to selectins [12,13,14,15]. We have previously shown that the N-terminal region of human PSGL-1 (amino acids 42–61) containing a potential *O*-glycosylation residue (T57) and three

Author Summary

Enterovirus 71 (EV71) is a major causative agent of hand, foot, and mouth disease and a diverse array of neurological diseases, including fatal encephalitis, in children. EV71 has increasingly caused large outbreaks of hand, foot, and mouth disease particularly in the Asia-Pacific region. Recently, we identified human P-selectin glycoprotein ligand-1 (PSGL-1) as a functional receptor for EV71. PSGL-1 on immune cells is a key molecule involved in early inflammatory events and the PSGL-1–selectin interaction is regulated by post-translational modifications of PSGL-1. Here, we found that a post-translational modification, tyrosine sulfation, at the N-terminal region of PSGL-1 is critical for its binding to EV71 and subsequent viral replication in lymphocytes. Important roles for tyrosine sulfation in protein-protein interactions have been widely accepted; however, involvement of tyrosine sulfation of the receptor in the virus-receptor interaction has been reported only for HIV-1. Therefore, this is the second and unique example of the involvement of tyrosine sulfation in specific virus-receptor interactions. Our results shed new light on biological roles for tyrosine-sulfated proteins in cell tropism and the pathogenesis of EV71.

potential tyrosine sulfation sites (Y46, Y48, and Y51) is directly responsible for PSGL-1 binding to EV71-PB [5]. Therefore, in the present study, we investigated the involvement of post-translational modifications of PSGL-1 in the binding to EV71-PB using a series of PSGL-1 mutants and an inhibitor of sulfation.

Tyrosine sulfation is an important late post-translational modification of secreted and membrane-bound proteins expressed in various mammalian cells and tissues and occurs in the trans-Golgi network [16,17]. Tyrosine sulfated proteins have been described in many mammalian species, and important roles for tyrosine sulfation in protein-protein interactions have been widely accepted, particularly for various chemokine receptors and their ligands that mediate leukocyte migration during inflammation. Furthermore, it has been well established that tyrosine sulfation of the N-terminal region of the chemokine receptor, C-C chemokine receptor 5 (CCR5), plays critical roles in the function of CCR5 as a coreceptor for virus entry and replication of CCR5-tropic human immunodeficiency virus type 1 (HIV-1) variants [18].

Here we demonstrate that tyrosine sulfation of the N-terminal region of PSGL-1 facilitates PSGL-1–EV71 interaction and viral replication of EV71-PB in Jurkat T cells. To our knowledge, this is the second direct example of the involvement of tyrosine sulfation in specific virus-receptor interactions, a modification that mediates viral entry and replication in target cells.

Results

O-glycosylation at T57 of PSGL-1 is not necessary for EV71-1095 binding

For binding to selectins, PSGL-1 requires post-translational modifications with sialyl Lewis x-containing *O*-glycans at T57. α1,3-fucosyltransferase (FUT7) is involved in the biosynthesis of sialyl Lewis x determinants (Fig. 1A) [19,20]. Prevention of *O*-glycosylation by alanine substitution at T57 (T57A) eliminates binding of PSGL-1 to P-selectin without affecting tyrosine sulfation [12]. First, we generated and expressed a PSGL-1-T57A mutant (Fig. 1A) in 293T cells (293T/T57A) to examine the role of *O*-glycosylation on T57 for PSGL-1 binding to EV71-1095, a representative strain of EV71-PB [5]. As a positive binding control, we used a soluble form of recombinant P-selectin (P-selectin-Fc). P-selectin-Fc did not bind to any PSGL-1 transfectants in the presence of 2 mM EDTA (Fig. 1B). P-selectin-Fc bound weakly to 293T cells transiently expressing PSGL-1 (293T/PSGL-1) in the presence of Ca^{2+} but not to 293T/T57A cells (Fig. 1B). Double expression of PSGL-1 and FUT7 in 293T cells resulted in the efficient binding of P-selectin-Fc to PSGL-1 in a calcium-dependent manner (Fig. 1B). Even in the presence of Ca^{2+} and FUT7, P-selectin-Fc did not bind to 293T/T57A cells (Fig. 1B). These observations are consistent with previous findings that interaction of PSGL-1 with P-selectin is calcium-dependent and requires appropriate *O*-glycosylation of PSGL-1 at T57 [10,12]. In contrast, EV71-1095 showed marked binding to 293T/PSGL-1 cells in a calcium-independent manner, even in the absence of FUT7 (Fig. 1B). EV71-1095 also bound to 293T/T57A cells (Fig. 1B). These results indicate that, unlike the interaction between PSGL-1 and P-selectin, the interaction between PSGL-1 and EV71-1095 does not require Ca^{2+} and the *O*-glycans at T57 of PSGL-1.

Sialic acids are not necessary for EV71-1095 binding

To examine the role of sialic acids on the cell surface, including sialyl Lewis x moieties in the potential *O*-glycans at T44 and T57 of PSGL-1, on EV71 binding to 293T/PSGL-1 cells, we tested EV71 binding to the cells pretreated with sialidase. Sialidase treatment removed cell-surface sialyl Lewis x (Fig. 2A) and reduced P-selectin-Fc binding to 293T/PSGL-1 cells (Fig. 2B). On the other hand, EV71-1095 binding to the sialidase-treated cells was not reduced regardless of the removal of sialyl Lewis x (Fig. 2C). Although treatment with sialidase decreased EV71 infection to DLD-1 cells [21], sialic acids on the cell surface of 293T/PSGL-1 cells are not necessary for the binding of PSGL-1 to EV71-1095.

An inhibitor of sulfation reduces PSGL-1 binding to EV71-PB

In addition to *O*-glycosylation of PSGL-1, sulfation of the three tyrosines (Y46, Y48, and Y51) in the N-terminal region of PSGL-1 is required for high affinity binding to P- and L-selectins [13,14,15,22,23]. To assess the role of tyrosine sulfation of PSGL-1 in the PSGL-1–EV71 interaction, we treated 293T/PSGL-1 cells with sodium chlorate, an inhibitor of sulfation that blocks PSGL-1 binding to P-selectin [13]. As described previously, sodium chlorate had no apparent effect on PSGL-1 expression on the cell surface (Fig. 3A). On the other hand, sodium chlorate reduced sulfated tyrosines on the cell surface (Fig. 3B) and inhibited EV71-1095 binding to 293T/PSGL-1 cells in a dose-dependent manner (Fig. 3C). These observations indicated that sulfation of PSGL-1, in addition to its expression on the cell surface, is important for EV71 binding.

One or more tyrosines in the N-terminal region of PSGL-1 are important for EV71-PB binding

We then determined the requirement for the putative sulfated tyrosines (Y46, Y48, or Y51) in the N-terminal region of PSGL-1 for its binding to EV71-1095. We generated PSGL-1 mutants with phenylalanine substitutions at one or more tyrosines and a mutant with a deletion of this region (Fig. 4A). We transfected 293T cells with expression plasmids containing the PSGL-1 mutants and used them for the EV71 binding assay using flow cytometry. 293T cells transfected with an empty vector expressed little or no detectable tyrosine sulfated proteins on the cell surface (Fig. 4B). Similar to the binding of PSGL-1 to P-selectin [13,14], substitution of the tyrosines with phenylalanine prevented tyrosine sulfation and

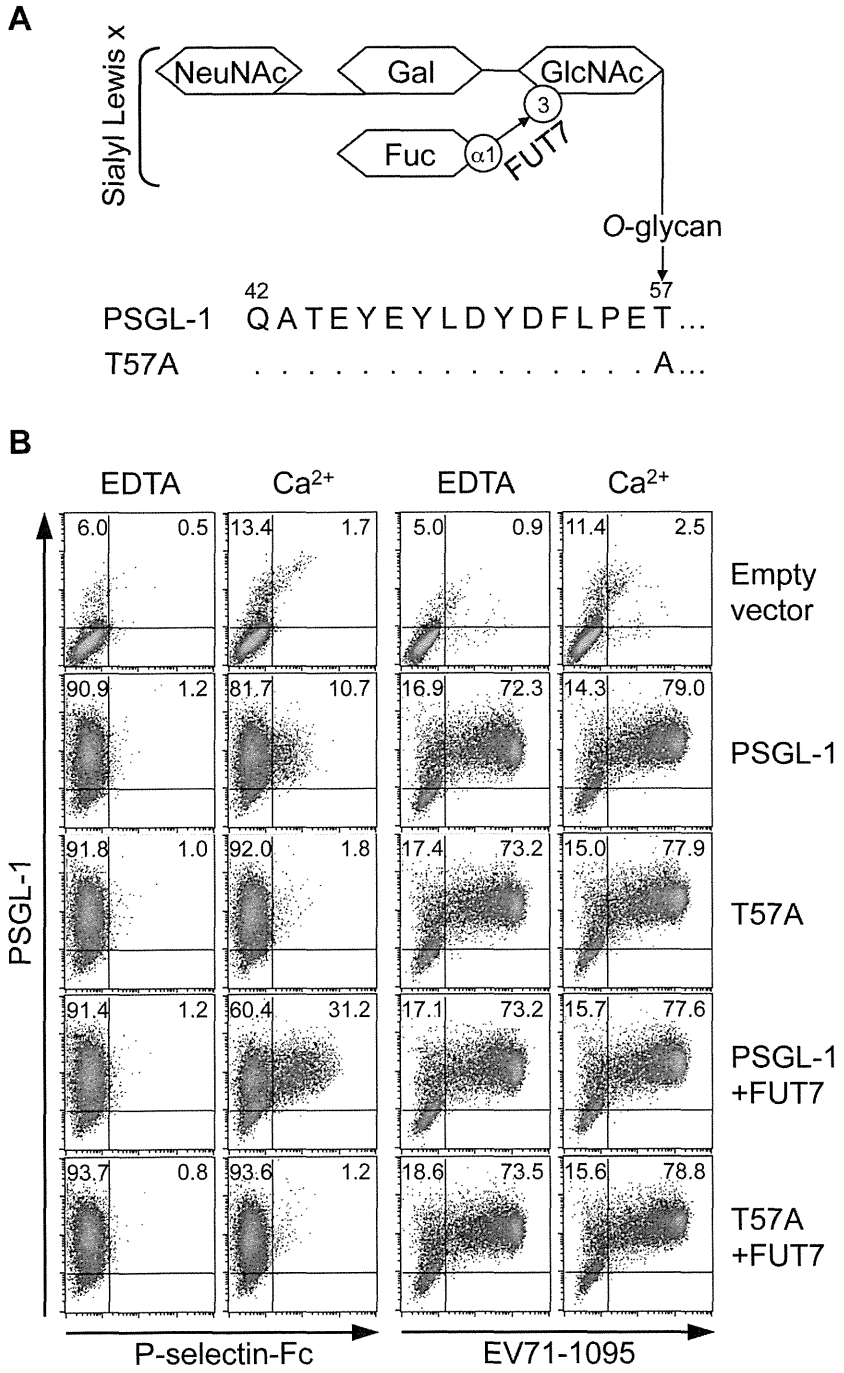

Figure 1. PSGL-1 *O*-glycosylation at T57 is not necessary for binding to EV71-1095. (A) Schematic structure of the *O*-glycosylation of PSGL-1 and the T57A mutant. FUT7 is involved in the synthesis of sialyl Lewis x. (B) 293T cells were transfected with the indicated expression plasmids. Transfectants were incubated with P-selectin-Fc or EV71-1095 in the presence (Ca^{2+}) or absence (EDTA) of 2 mM $CaCl_2$ followed by the P-selectin-Fc or EV71 binding assay using flow cytometry. The percentage of cells bound to P-selectin-Fc or EV71-1095 is indicated in the upper right quadrant. The data are representative of three independent experiments.
doi:10.1371/journal.ppat.1001174.g001

PSGL-1 binding to EV71-1095 (Fig. 4B). Substitution of one or two tyrosines slightly reduced (Y46F) or impaired (Y48F, Y51F, Y4648F, or Y4651F) the binding of PSGL-1 to EV71-1095 regardless of the apparent expression of tyrosine sulfated proteins on the cell surface (Fig. 4B). Substitution of two or three tyrosines (Y4851F or FFF) or deletion of the region (d46–51) reduced tyrosine sulfated proteins on the cell surface and completely disrupted the PSGL-1–EV71 interaction (Fig. 4B). We also examined the role of tyrosine sulfation in PSGL-1 binding to other EV71-PB strains. Binding of SK-EV006, C7/Osaka, KED005, and 75-Yamagata strains to 293T/PSGL-1 cells was also inhibited by sodium chlorate (Fig. S1). These strains bound to 293T/T57A cells but not to 293T cells expressing the PSGL-1-FFF mutant. Taken together, these findings demonstrate that, in contrast to *O*-glycosylation at T57, tyrosine sulfation of PSGL-1 is essential for the efficient binding to EV71-PB strains.

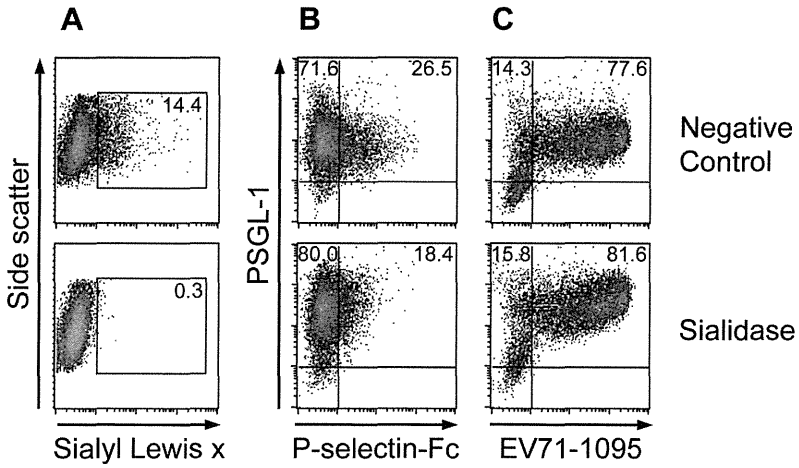

Figure 2. Effect of sialidase treatment on PSGL-1 binding to EV71-1095. (A) Sialyl Lewis x expression on the cell surface, as measured with flow cytometry. The percentage of cells expressing sialyl Lewis x is indicated. (B) The cells were examined with the P-selectin-Fc binding assay using flow cytometry. The percentage of cells bound to P-selectin-Fc is indicated in the upper right quadrant. (C) The cells were examined with the EV71 binding assay using flow cytometry. The percentage of cells bound to EV71-1095 is indicated in the upper right quadrant. As a negative control, 293T/PSGL-1 cells were incubated in the medium without sialidase. The data are representative of three independent experiments.
doi:10.1371/journal.ppat.1001174.g002

Sodium chlorate inhibits EV71-PB replication in Jurkat T cells

We next examined whether sulfation of PSGL-1 is required for PSGL-1-dependent replication of EV71-PB in Jurkat T cells. Jurkat T cells were infected with EV71 and cultured in the presence of sodium chlorate to inhibit the sulfation of PSGL-1. Sodium chlorate treatment did not affect PSGL-1 expression on Jurkat T cells (Fig. 5A). On the other hand, sodium chlorate significantly inhibited the replication of EV71-1095 in a dose-dependent manner (Fig. 5B). The replication of other EV71-PB strains was also inhibited in the presence of sodium chlorate (Fig. 6). In contrast, replication of EV71-non-PB strains (EV71-02362 and EV71-Nagoya), which can replicate in Jurkat T cells in a PSGL-1-independent manner [5], was not affected by sodium chlorate (Figs. 5C and 6). This observation supports that sodium chlorate inhibited replication by blocking EV71-PB entry into the cells. To confirm that sodium chlorate is acting at the receptor level, we transfected Jurkat T cells with genomic RNA of EV71-

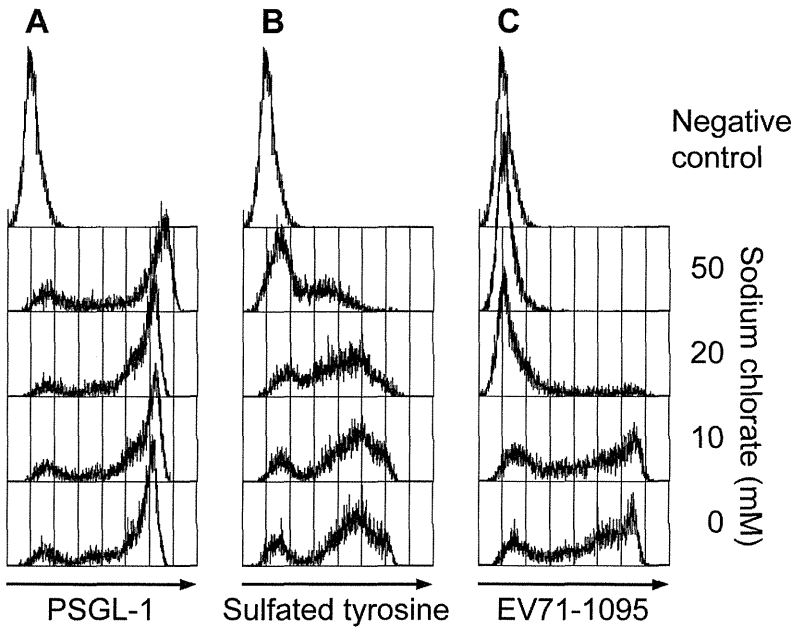

Figure 3. Effect of sodium chlorate on PSGL-1 binding to EV71-1095. Pretreatment of 293T/PSGL-1 cells with sodium chlorate reduces EV71-1095 binding in a dose-dependent manner. (A) PSGL-1 expression on the cell surface, as measured with flow cytometry. As a negative control, 293T/PSGL-1 cells cultured in the absence of sodium chlorate were stained with an isotype control antibody. (B) Sulfated tyrosines on the cell surface, as measured with flow cytometry. As a negative control, 293T/PSGL-1 cells cultured in the absence of sodium chlorate were stained with an isotype control antibody. (C) The cells were examined with the EV71 binding assay using flow cytometry. As a binding control, 293T/PSGL-1 cells were treated with mock-infected culture supernatant. The data are representative of three independent experiments.
doi:10.1371/journal.ppat.1001174.g003